La mer 63 : 57–94, 2025, https://doi.org/10.32211/lamer.63.3-4_57
Société franco-japonaise d'Océanographie, Tokyo

ASUKA: Observing the Kuroshio south of Japan for estimating volume transport

Shiro IMAWAKI[1)] *

Abstract: The Affiliated Surveys of the Kuroshio off Cape Ashizuri (ASUKA) Group conducted intensive observation of the Kuroshio off Shikoku over a two-year period (1993–1995), by current-meter moorings and frequently repeated hydrographic surveys, with the primary objective of estimating volume transport. This review paper describes the observational program and summarizes the major findings obtained from the ASUKA dataset and its combination with satellite altimetry data. A very strong vertical velocity shear was observed in the upper Kuroshio during the nearshore path, whereas a very weak shear was observed in the upper coastal countercurrent during the offshore path. Geostrophic balance was confirmed to hold well in intermediate and deep layers, as indicated by excellent agreement in vertical difference between geostrophic and measured velocities. From eight full-depth geostrophic velocity sections referred to velocities measured at mid-depths, the average volume transport of the Kuroshio was estimated at 60 Sv (1 Sv = 10^6 m^3 s^{-1}) and that of the throughflow Kuroshio, excluding the contribution of a local offshore anticyclonic eddy, was estimated at 44 Sv. A strong linear relationship was found between net transport integrated from the coast and sea-surface dynamic topography difference from the coast. Using this relationship, satellite altimetry data enabled us to derive proxy time series of transport for the past three decades, yielding means of 61 Sv for the Kuroshio and 35 Sv for the throughflow Kuroshio. The mean transport of the throughflow Kuroshio during large meander periods was nearly identical to that during non-large meander periods. Beneath the Kuroshio, a pair of stable deep westward and eastward flows, intensifying toward the bottom, was observed over the Nankai Trough.

Keywords : ASUKA, Kuroshio, moored current-meter, satellite altimetry, volume transport

1. Introduction

The moderate climate of the Earth is maintained through meridional heat transport by both the oceans and the atmosphere (e.g., BRYDEN and HALL, 1980; TALLEY, 1984; MACDONALD and WUNSCH, 1996). In the North Atlantic, the deep meridional overturning circulation plays a fundamental role in net heat transport (e.g., MACDONALD and BARINGER, 2013). Conversely, in the North Pacific, net meridional heat transport is primarily caused by upper-layer circulation, making the wind-driven horizontal circulation important (e.g., BRYDEN et al., 1991; MACDONALD

1) Professor Emeritus of Kyushu University, Yokohama, 224–0014, Japan
*Corresponding author:
E-mail: imawaki@g04.itscom.net

and BARINGER, 2013). Accordingly, the western-boundary current of the wind-driven subtropical gyre of the North Pacific, i.e., the Kuroshio, plays a vital role by transporting warm water northward, thereby compensating for the southward transport of cooler water in the ocean interior.

Until the early 1990s, velocity of the Kuroshio had not been measured accurately due to technical difficulties of velocity measurements within a strong current. Most information about velocity and volume transport relied on geostrophic calculations based on the assumption of no motion at a chosen deep reference level. The resulting volume transport is referred to as geostrophic transport (GT). When geostrophic velocity and transport are referred to measured or inferred velocities at the reference level, they are termed absolute geostrophic velocity (AGV) and absolute geostrophic transport (AGT), respectively.

The following are pioneering studies on current measurements of the Kuroshio near Japan. WORTHINGTON and KAWAI (1972) conducted direct current measurements in the deep layer in 1965 by tracking neutrally-buoyant floats and estimated AGTs of the Kuroshio for the first time. They reported AGTs of 84 Sv ($1\ \mathrm{Sv} = 10^6\ \mathrm{m}^3\ \mathrm{s}^{-1}$) south of Shikoku and 88 Sv southeast of Cape Inubo. TAFT (1978) deployed current-meters (CMs) near the bottom for the first time in 1971 and estimated AGTs of 70 Sv east of Kyushu, 57 Sv south of Shikoku, and 77 Sv south of Honshu. TAKEMATSU et al. (1986) used moored CMs to measure surface-layer velocities of the Kuroshio south of Kyushu from 1979 to 1983. Their results showed that the Kuroshio was confined to the upper 600 m layer, on average, at this location, suggesting that a reference level of no motion in geostrophic calculations should be selected with caution. KANEKO et al. (1992) measured velocity across the Kuroshio south of Shikoku and Honshu down to 400 m depth using an acoustic Doppler current profiler (ADCP) towed from a ship (towed-ADCP). Their observation revealed a subsurface velocity core of the Kuroshio and a subsurface countercurrent.

Volume transport of the Kuroshio has been estimated from hydrographic surveys conducted south of Japan (e.g., SUGIMOTO et al., 2010; NAGANO et al., 2013; LONG et al., 2018) and in the Tokara Strait (e.g., GUO et al., 2012; WEI et al., 2013; LIU et al., 2019). For hydrographic sections that form a closed volume, velocities at reference levels can be inferred using the inverse method developed by WUNSCH (1978), which has been applied to the Kuroshio region to estimate AGTs (e.g., NAKANO et al., 1994; KANEKO et al., 2001; ZHU et al., 2006; NAGANO et al., 2010; GUO et al., 2013). A detailed review of Kuroshio-related studies was given by ANDO et al. (2021).

The large international program, the World Ocean Circulation Experiment (WOCE), began an eight-year observational campaign in 1990. Its primary objective was to observe the three-dimensional structure of the global ocean to provide a basis for improving ocean models, and by extension, to improve the reliability of climate models (GRASSL, 2001). The Kuroshio south of Japan was identified as an important observational target, and its associated current measurement array was designated PCM5 (SIEDLER et al., 2001). The array was intended to be combined with a trans-Pacific hydrographic survey along 30° N (WOCE Hydrographic Program P2) to estimate the net meridional heat transport at mid-latitudes in the North Pacific.

The altimetry satellite TOPEX/Poseidon began measuring sea-surface height in September 1992, with the objective of improving understanding of global ocean circulation (FU et al., 1994). Satellite remote-sensing was a key contributor to the success of WOCE (SIEDLER et al., 2001). Altimetric measurements have since been continued along the same subsatellite track by its successor Jason-1 and others (e.g., ESCUDIER et al., 2017).

The PCM5 observation by means of CM moorings and frequently repeated hydrographic surveys were conducted from 1993 to 1995 by the Affiliated Surveys of the Kuroshio off Cape Ashizuri (ASUKA) Group, being hereafter referred to as the ASUKA intensive observation (Fig. 1). The primary objective of this observation was to estimate the AGT of the Kuroshio as accurately as possible (IMAWAKI et al., 1997). Its observation line was aligned with subsatellite track number 112 of TOPEX/Poseidon, which passes over Cape Ashizuri (see Fig. 1 in UCHIDA and IMAWAKI, 2008), thereby facilitating the integration of *in situ* and altimetry data. As a result, the ASUKA intensive observation was the largest-scale measurement program of the Kuroshio south of Japan. Also the ASUKA program was considered to be the most comprehensive effort of western-boundary current observation during the WOCE period, providing a multiyear transport record through a combination of *in situ* current measurements, geostrophy, and satellite altimetry (CLARKE et al., 2001). During the intensive observation period, the Kuroshio took the non-large meander path as classified by KAWABE (1995), as indicated by IMAWAKI et al. (2023), which is hereafter abbreviated as IM23.

As shown in the inset of Fig. 1, the Kuroshio enters the Shikoku Basin from the East China Sea through the Tokara Strait and merges with the Ryukyu Current to the east of the Strait. In the Shikoku Basin, the Kuroshio usually flows along the southern coast of Japan, accompanied by the local anticyclonic stationary eddy on its offshore side (HASUNUMA and YOSHIDA, 1978), which is known as the Warm Eddy off Shikoku. The transport of the eastward-flowing, nearshore-side half of the Warm Eddy is necessarily included in transport of the Kuroshio as the whole eastward flow, which is hereafter referred to as the Kuroshio. The westward-flowing, offshore-side half is referred to as the Kuroshio recirculation and must be accounted for when estimating the net transport of the Kuroshio as throughflow, which is hereafter referred to as the throughflow Kuroshio. The throughflow transport is defined as the transport of the Kuroshio minus the transport of the Kuroshio recirculation.

Major findings from the ASUKA program have been published in various journals. This review provides a comprehensive summary of those results as well as a detailed description of the ASUKA field observation. The structure of rest of the paper is as follows. Section 2 describes the ASUKA intensive observation and satellite altimetry data used. Section 3 presents the primary outputs of the intensive observation, including descriptions of the flow field and estimates of volume transport. Section 4 shows observations and studies following the intensive phase. Section 5 introduces the time series of volume transport derived from the combined ASUKA and altimetry data. Sections 6 and 7 present the discussion and summary, respectively.

2. Intensive observation and altimetry data

Figure 1 shows the ASUKA observation line, consisting of hydrographic stations and mooring stations in the Kuroshio and Kuroshio recirculation regions off Shikoku, Japan. The line is oriented approximately perpendicular to the typical path of the Kuroshio off Cape Ashizuri, where the current path is most stable within the Shikoku Basin (TAFT, 1972). In the Kuroshio region (north of 30° N), the spacing of coordinated common hydrographic stations was either 20 or 31 km, while mooring stations were spaced at intervals ranging from 20 to 92 km. On the continen-

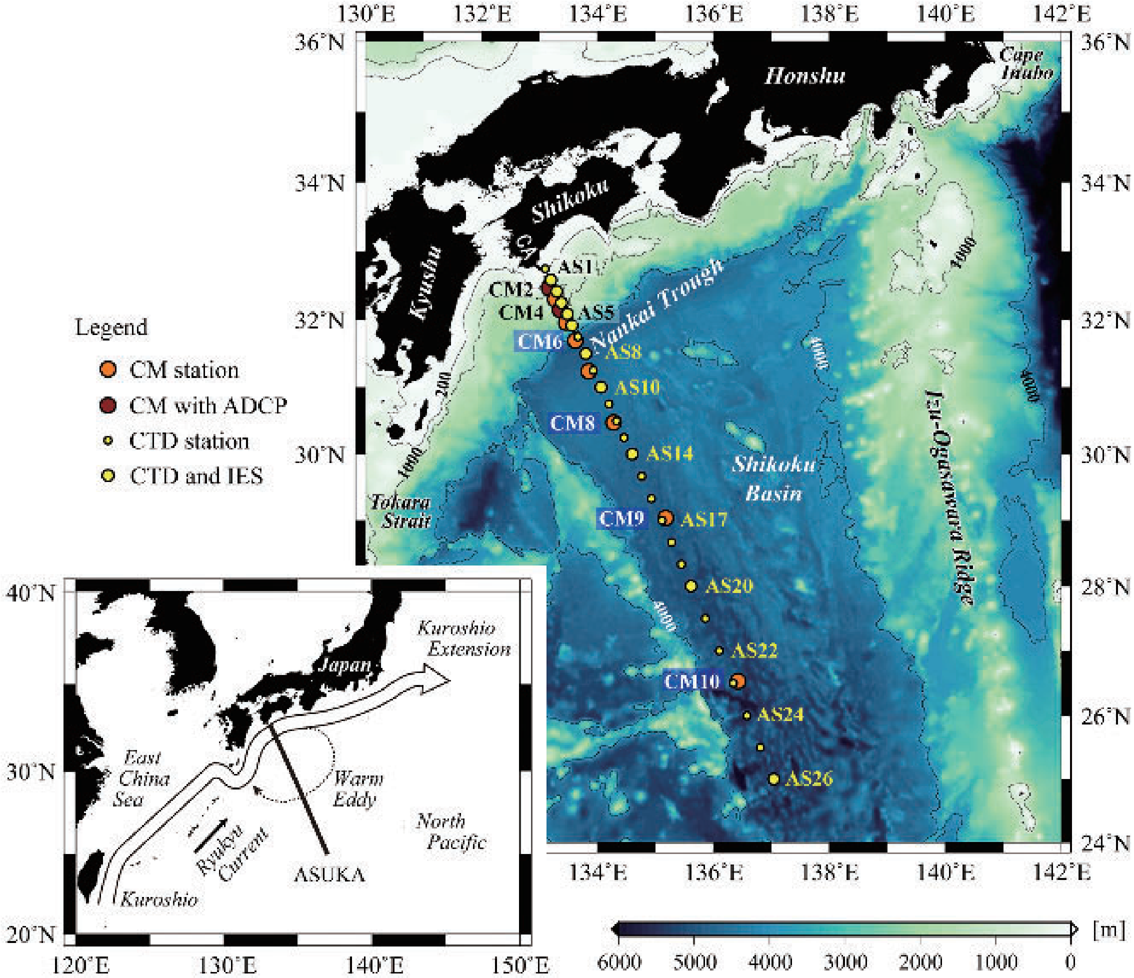

Fig. 1 The ASUKA (Affiliated Surveys of the Kuroshio off Cape Ashizuri) observation line (155° True), crossing the Kuroshio off Shikoku, Japan. Coordinated common hydrographic stations (AS1–AS26; yellow dots and circles) and mooring stations (CM2–CM10; orange and maroon circles) are shown on a map of bottom topography based on Amante and Eakins (2009). Two maroon circles (CM2 and CM4) show mooring stations equipped with an upward-looking ADCP (acoustic Doppler current profiler). Ten yellow circles show IES (inverted echo sounder) stations. The location of Cape Ashizuri is shown by CA in Shikoku. The small-scale inset shows the ASUKA line relative to the schematic flow pattern of the Kuroshio and the Warm Eddy off Shikoku. Adapted from Imawaki et al. (2023)

tal slope, mooring stations were positioned halfway between hydrographic stations. To prevent entanglement between conductivity-temperature-depth recorder (CTD) cables and mooring lines, mooring stations were offset by about 7 km upstream of hydrographic stations. To include the Kuroshio recirculation in transport estimates, the observation line was extended southward to 25° N.

Figure 2 shows the vertical distribution of moored instruments. Aanderaa CMs (primarily model RCM-5) were deployed at nominal depths

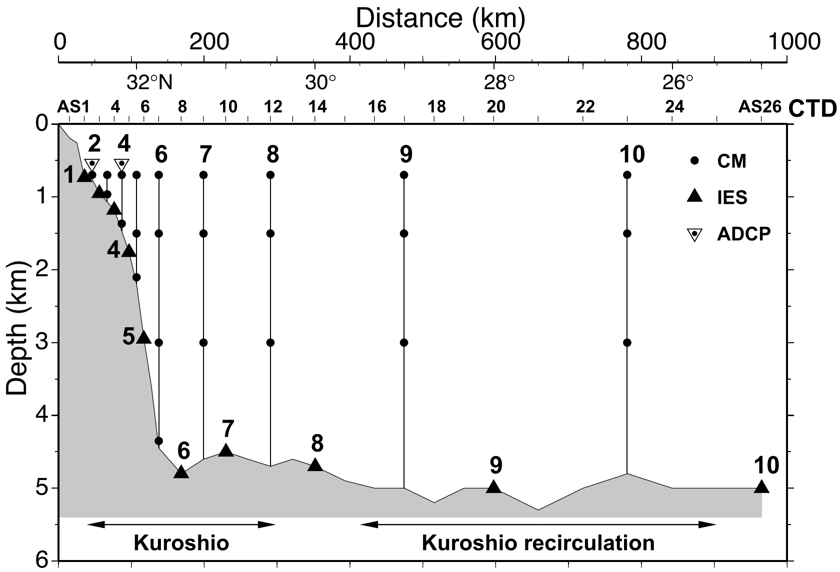

Fig. 2 Locations and nominal depths of deployed instruments, including CMs (current-meters), upward-looking ADCPs and IESs. Tick marks at the top denote locations of coordinated common hydrographic stations (CTD; AS1–AS26). The shaded area represents ocean bottom. From IMAWAKI et al. (1997).

of 700, 1500, and 3000 m, and near the bottom. The CMs measured temperature as well as current speed and direction. Two CMs were deployed at the 700 m level, as this depth was considered the most important for providing velocities at the reference level. CMs were also deployed on the continental slope to detect near-bottom flows. Upward-looking ADCPs (moored-ADCPs) were installed at the tops of mooring lines at Stations CM2 and CM4 to capture the strong current of the upper-layer Kuroshio, which could not be measured by standard moored CMs. Inverted echo sounders (IESs) were deployed on the bottom such that each CM station was positioned halfway between adjacent IES stations, to infer upper-layer fields of temperature and AGV continuously, thereby supplementing the sporadic hydrographic surveys.

The ASUKA intensive observation was initiated in October 1993 with the deployment of nine moorings equipped with 33 CMs (UMATANI et al., 2001; KASHIMA et al., 2003) and two moored-ADCPs (TAKEUCHI et al., 2002), and ten IESs (BOOK et al., 2002a; 2002b). Mooring lines were deployed by the buoy-first, anchor-last method. In September 1994, the nine moorings were recovered and redeployed with the same configurations. The final recovery of all moorings and IESs was conducted in November 1995, marking the end of the intensive observation. All of the instruments were successfully recovered, with the exception of four CMs from the second-year deployment at Station CM8 and the IES at Station IES5.

Actual instrument depths differed from their designed ones, mostly because moorings were deployed at depths different from planned ones unavoidably, especially at stations on the continental slope, and partly because mooring lines were titled in the strong current. To monitor instrument depths, pressure was measured by CMs at the nominal depth of 700 m. For example, their mean depths at Stations CM2 through CM7 were estimated at 530–690 m.

During the intensive observation period, the ASUKA Group conducted hydrographic surveys along the observation line using CTDs, expendable CTDs, and expendable bathy-thermographs (XBTs) as frequently as possible (UCHIDA et al., 2008). In total, 42 hydrographic sections were obtained for the upper 1000 m in the Kuroshio region. Eight of them were full-depth CTD sections (IM23). In addition, velocity measurements using a towed-ADCP were carried out 12 times along the ASUKA line (ZHU et al., 2001).

This ASUKA intensive observation was conducted by a collaborative group of a large number of scientists from Japan and the United States of America (IMAWAKI et al., 2001; BOOK et al., 2002a). This large-scale observation was not organized under a single project but was made possible through the coordinated efforts of many scientists from universities, research institutes, and agencies. The scale and success of the observation likely reflect the common deep interest of many Japanese physical oceanographers in the Kuroshio.

Altimetric sea-level anomalies along the TOPEX/Poseidon subsatellite track were used to derive proxy time series of Kuroshio volume transport (IMAWAKI et al., 2001; UCHIDA, 2025). Gridded sea-surface dynamic topography (SSDT) data derived from satellite altimetry were used to examine horizontal flow patterns of the Kuroshio and its recirculation (IM23; IMAWAKI et al., 2025). These altimetry data were produced by the SSALTO Multimission Ground Segment/Data Unification and Altimeter Combination System (AVISO, 2016), and provided by the Archiving, Validation, and Interpretation of Satellite Oceanographic Data (France) and the Copernicus Marine Service Information (European Union). Additionally, sea-level data from the tide gauge at Cape Ashizuri (see Fig. 1 for location), maintained by the Japan Meteorological Agency, were used as a reference for the altimetric sea-level profile along the ASUKA line (IMAWAKI et al., 2001; UCHIDA, 2025).

3. Results from intensive observation

Representative examples of vertical sections of potential temperature, salinity, and AGV in the Kuroshio and Kuroshio recirculation regions are shown in Fig. 3. The velocity component perpendicular to the ASUKA line, oriented toward 65° True, is hereafter referred to simply as velocity. Mean vertical sections of potential temperature and salinity, based on 154 sections collected from 1992 to 2008, were provided by UCHIDA et al. (2008). These sections reveal following features. The 10° C isotherm, which indicates the center of the main thermocline, deepens from approximately 300 m near the coast to 650 m offshore (at 30–31° N). The main body of the Kuroshio is located near the coast, as indicated by the pronounced inclination of the main thermocline and AGV values exceeding 10 cm s^{-1}. The core of the North Pacific Intermediate Water, which is characterized by a vertical salinity minimum, deepens from approximately 500 m near the coast to 800 m offshore (at 31° N). The core of the North Pacific Subtropical Mode Water, which is characterized by a vertical salinity maximum, is located at around 150 m on the offshore side of the Kuroshio. The instantaneous AGV section (Fig. 3 (c)) shows complex eastward and westward flows associated with active mesoscale eddies in the Kuroshio recirculation region.

The validity of geostrophic balance in the Kuroshio and Kuroshio recirculation regions was examined using repeated hydrography data and moored CM data at nominal depths of 700, 1500,

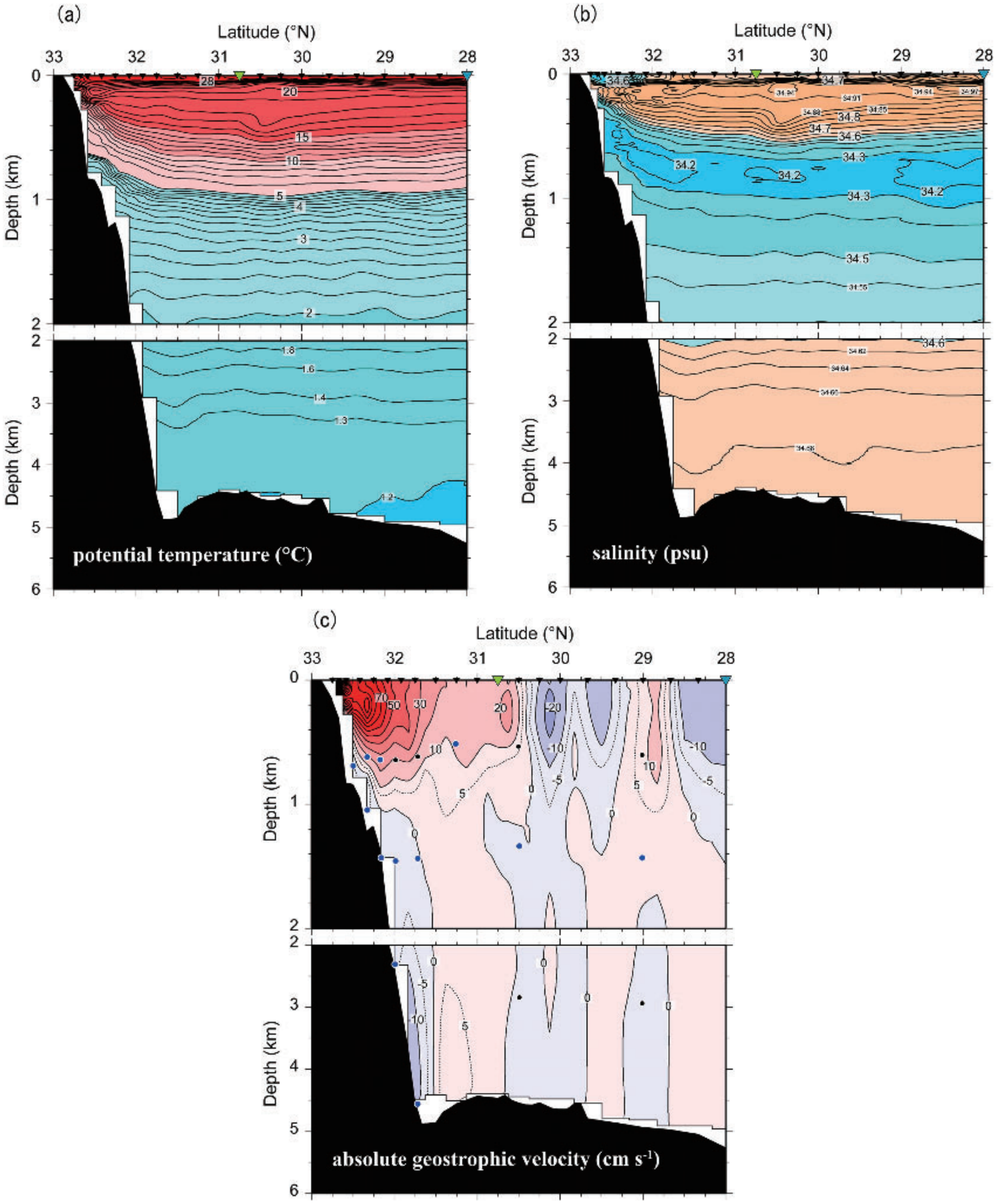

Fig. 3 Vertical sections along the ASUKA line in September 1994 of (a) potential temperature, (b) salinity, and (c) AGV (absolute geostrophic velocity; component toward 65° True); southern parts (25–28° N) are not shown. Triangles at the top denote locations of hydrographic stations; the yellowish green triangle marks the inferred offshore edge of the Kuroshio, and the light blue triangle marks the inferred southern end of the Kuroshio recirculation. In (c), dots denote locations of moored CMs; larger blue ones indicate CMs providing velocities at reference levels or on the continental slope. Courtesy of Hiroshi Uchida.

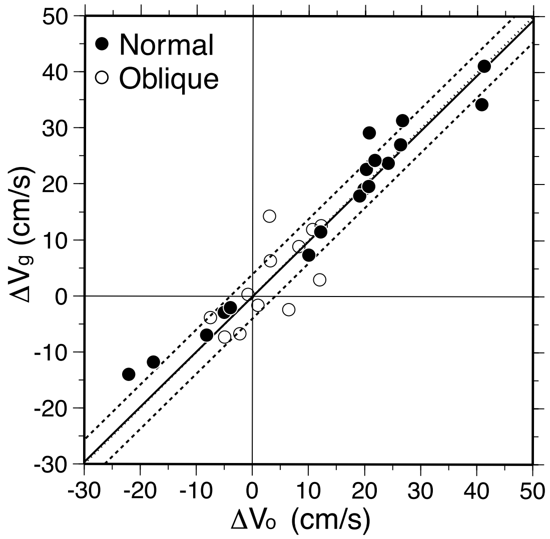

Fig. 4 Scatter plot of vertical differences of estimated geostrophic velocity (ΔVg) versus measured velocity (ΔVo) between nominal depths of 700 and 1500 m. Cases were classified as "normal" when the current direction at 700 m depth was approximately perpendicular to the ASUKA line, and as "oblique" when it was approximately parallel; the sorting criterion was 45°. The solid line denotes the regression line through the origin for 18 normal cases; dashed lines denote the root-mean-square difference from the regression line. The almost hidden dotted line denotes the one-to-one relation. Adapted from KASHIMA et al. (2003).

and 3000 m (KASHIMA et al., 2003). For these depth intervals, vertical differences of geostrophic velocity were compared with corresponding differences of measured velocity. Figure 4 shows the results for the intermediate layer (between nominal depths of 700 and 1500 m), where vertical differences ranged from −20 to 40 cm s^{-1}. The agreement was excellent for 18 comparisons of flows approximately perpendicular to the ASUKA line, with an almost one-to-one correspondence between the two values; the slope of regression line was 0.99, the correlation coefficient (CC) was 0.98, and the root-mean-square difference from the regression line was 2.8 cm s^{-1}, which was close to the estimated measurement error of 2.1 cm s^{-1}. For the deep layer (between nominal depths of 1500 and 3000 m), ten comparisons yielded corresponding values of 0.82, 0.93, 1.2 cm s^{-1}, and 2.0 cm s^{-1}. These results indicated that geostrophic balance holds very well in both the intermediate and deep layers. The best agreement was obtained when measured velocities were averaged over several days. In contrast, geostrophic balance may break down in the upper-layer near the coast, particularly when strong vertical velocity shear is induced abruptly. This condition is shown in the next subsection.

The accuracy of SSDT from the altimetry satellite TOPEX/Poseidon was examined using AGV data during 1993–1994 (IMAWAKI and UCHIDA, 1995). In physical oceanography, only anomalies from an unknown mean SSDT are useful in satellite altimetry data. This unknown mean was estimated by minimizing the difference between altimetric SSDT and *in situ* SSDT obtained simultaneously. The *in situ* SSDT was derived by horizontally integrating the sea-surface AGV, referred to the nearshore-most station (AS1), under the assumption of geostrophy. The AGV was referred to velocity measured at the 700 m level. Ten estimates of the unknown mean SSDT were averaged to obtain the final estimate. The resulting total SSDT profiles along the ASUKA line north of 30° N showed good agreement with the *in situ* SSDT profiles, having an average root-mean-square difference of 4.6 cm.

3.1 Flow field of the Kuroshio

The following features of the flow field of the Kuroshio were identified using four different types of datasets: current vectors at nominal depths of 700, 1500, and 3000 m measured by moored CMs at nine stations (UMATANI et al.,

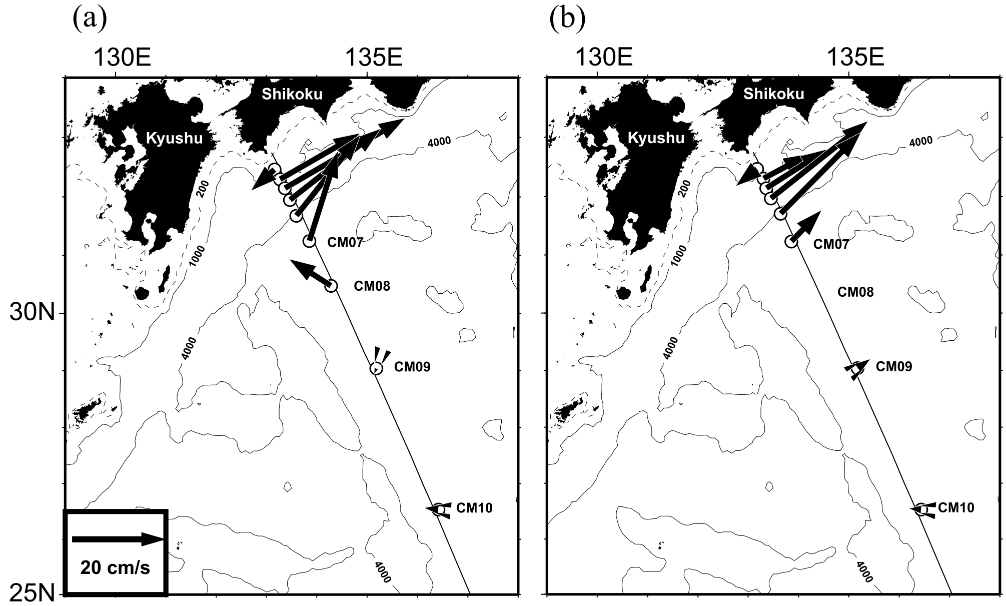

Fig. 5 Horizontal distributions of one-year mean current vectors measured at the nominal depth of 700 m. (a) First deployment (1993–1994), and (b) second deployment (1994–1995). From UMATANI et al. (2001).

2001); velocities from approximately 300 to 500 m depth measured by moored-ADCPs at two stations (TAKEUCHI et al., 2002); 12 velocity sections along the ASUKA line, from the sea-surface to 400 m depth, measured by the towed-ADCP (ZHU et al., 2001); and eight full-depth AGV sections along the ASUKA line (IM23).

Horizontal distributions of one-year mean current vectors obtained from CMs at the 700 m level are shown in Fig. 5. The strongest part of the Kuroshio, hereafter referred to as the Kuroshio axis, was located at Station CM4 during the first deployment and at Station CM5 during the second deployment, both around 32° N, with speed of 30 and 28 cm s^{-1}, respectively. Current vectors near the Kuroshio axis were oriented nearly perpendicular to the ASUKA line, confirming that the line was, on average, aligned normal to the Kuroshio flow. A tendency toward convergence was observed on the offshore side of the Kuroshio at this depth. Vertical sections of annual-mean velocity derived from moored CMs indicated that the 10 cm s^{-1} contour associated with the Kuroshio extended down to 1000 m depth.

Time series of daily current vectors at the 700 m level at all stations are shown in Fig. 6 (a). These vectors exhibited marked fluctuations, which were nearly in phase at Stations CM3 through CM6. Daily current vectors at the 1500 m level were similar to those at the 700 m level, but weaker. At the 3000 m level, currents were generally very weak and showed no apparent correlation with those at the 700 m level, except at Station CM6, as discussed in Subsection 3.3.

During the intensive observation period, the Kuroshio took two distinct paths (i. e., a near-shore path and an offshore path), both of which are classified as the non-large meander path. Current vectors at 650 m depth were estimated

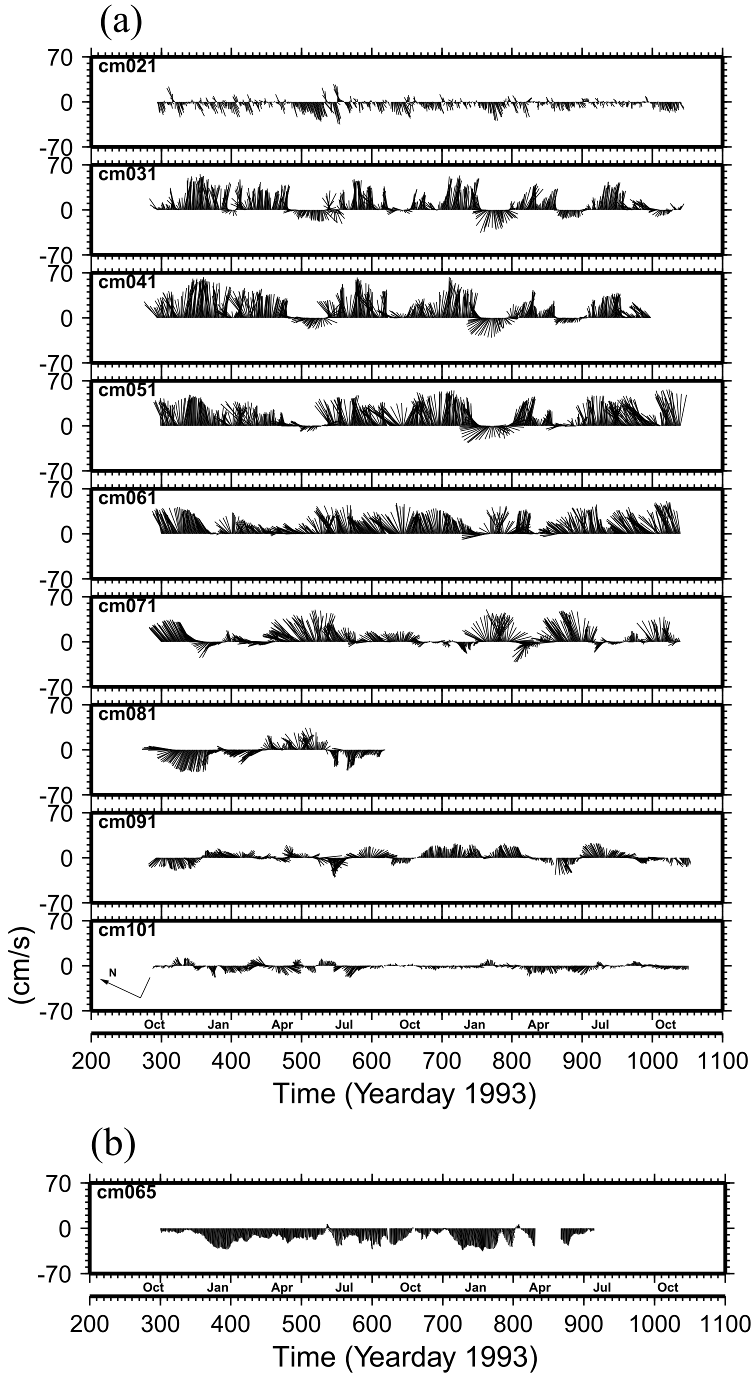

Fig. 6 Stick diagrams of daily current vectors measured during 1993–1995. The upward direction corresponds to 65° True, i.e., perpendicular to the ASUKA line. (a) Vectors at the nominal depth of 700 m at all the nine stations. (b) Vectors at 120 m above the bottom (4680 m depth) at Station CM6. From UMATANI et al. (2001).

by interpolating current vectors measured at nominal depths of 700 and 1500 m, where possible. A time-latitude plot of current speed at the 650 m depth showed that the Kuroshio took the offshore path on three occasions during the two-year period: May-June 1994, February-March 1995, and May-June 1995.

During the nearshore path, horizontally maximum velocities of the surface-layer (averaged over 0-250 m depth) observed by the towed-ADCP ranged from 80 to 150 cm s^{-1}. The Kuroshio axis was located at approximately 32° 20'N on average, as shown in Fig. 3 (a) of ZHU et al. (2001). Vertically maximum velocities near the Kuroshio axis were observed at subsurface (100-200 m depth). The moored-ADCP at Station CM2 (32° 28'N) near the coast recorded very strong velocities at 300 m depth intermittently, reaching 130-150 cm s^{-1} (Fig. 6 of TAKEUCHI et al., 2002). These strong flows were accompanied by an extremely strong vertical velocity shear between 300 and 400 m depth, reaching 1.5×10^{-2} s^{-1}. This is likely the strongest vertical velocity sheer ever directly measured in the Kuroshio. At the 650 m depth, daily velocities were up to 60 cm s^{-1}, and the Kuroshio axis was located at around 32° 05'N on average (Fig. 6 (b) of UMATANI et al., 2001). Both in the surface-layer and at the 650 m depth, the horizontal velocity shear was markedly stronger on the nearshore side than on the offshore side.

During the offshore path, horizontally maximum velocities of the surface-layer observed by towed-ADCP were approximately 100 cm s^{-1}, and the Kuroshio axis was located at 31° 20'N on average (Fig. 3 (a) of ZHU et al., 2001). At the 650 m depth, daily velocities were up to 50 cm s^{-1}, and the Kuroshio axis was located at approximately 31° 15'N (Fig. 6 (b) of UMATANI et al., 2001). At this depth, horizontal velocity shear was stronger on the nearshore side than on the offshore side, whereas in the surface-layer the velocity field was nearly symmetric with respect to the Kuroshio axis. The offshore path was characterized by remarkable countercurrents near the coast, which were the nearshore-side half of coastal cyclonic eddies associated with small meanders of the Kuroshio that originated southeast of Kyushu and propagated northeastward along the coast. The countercurrents, as observed by the two moored-ADCPs, were nearly barotropic and exhibited a very weak vertical velocity shear of 0.04×10^{-2} s^{-1} on average between 300 and 500 m depth (Fig. 8 of TAKEUCHI et al., 2002). The currents extended from the sea-surface to at least 700 m (Fig. 6 (a)), having a typical width of approximately 50 km and a mean velocity of approximately 20 cm s^{-1} (Fig. 2 of ZHU et al., 2001). Based on these values, their transport was roughly estimated at 3 Sv. These features of coastal countercurrents were also shown by time-depth diagrams of proxy AGV at Stations CM2, CM3, and CM4, derived from IES and moored CM data (KAKINOKI et al., 2008a).

In the Kuroshio recirculation region (Stations CM8 and CM9), fluctuations of daily current vectors at the 700 m level were considerably larger than their means (Fig. 6 (a)), implying that the recirculation was overwhelmed by active, propagating mesoscale eddies.

Velocities measured by the towed-ADCP (Fig. 2 of ZHU et al., 2001) are compared with those measured by moored-ADCPs (Figs. 4 and 6 of TAKEUCHI et al., 2002). A total of 18 comparisons are made: 12 at 300 m depth at Station CM2 and six at 380-390 m depth at Station CM4. The compared velocities range from − 30 to 110 cm s^{-1}. In all but one case, the difference between the measurement types is less than 20 cm s^{-1}; the exception is a 30 cm s^{-1} difference at 300 m depth at Station CM2, when the flow field changed rapidly. As a whole, they agree well with each other, with a very high CC of 0.96, although towed-ADCP velocities are slightly lower than moored-ADCP velocities, with a mean difference of 7 cm s^{-1}.

Eight full-depth AGV sections were obtained from hydrographic surveys, referred to velocities measured at the 700 m level over the continental slope and at the 1500 m level in the offshore region, as shown in Fig. 3 (c). All AGV sections are shown in Fig. S1 in the supplementary material of IM23. These sections indicated that the main body of the Kuroshio (defined as regions with AGV > 10 cm s^{-1}) was mostly confined to the upper 1000 m. Maximum velocities were observed in the upper 200 m north of 32° N, ranging from 60 to 150 cm s^{-1}. The Kuroshio recirculation was relatively weak and frequently dominated by propagating mesoscale eddies.

From the AGV sections, the offshore edge of the Kuroshio was inferred on the basis of the sign of AGT in the upper 1000 m between pairs of hydrographic stations. The inferred offshore edges corresponded closely with local maxima in SSDT along the ASUKA line (Fig. S2 in the supplementary material of IM23). On average, the offshore edge was located at 30° 50'N. In contrast, the southern end of the Kuroshio recirculation was not able to be determined using a similar method due to the influence of mesoscale eddies (Fig. S2 of IM23). Instead, it was inferred somewhat subjectively, with the aid of SSDT maps. The inferred southern end was located at 29° 20'N on average.

The estimated AGVs (Fig. S1 of IM23) are compared with velocities in the upper-layer (approximately 300–500 m depth) measured by moored-ADCPs (Fig. 6 of TAKEUCHI et al., 2002). The compared velocities range from 0 to 140 cm s^{-1}. At Station CM4 and below 400 m depth at Station CM2, the estimated velocities agree well with measured velocities within ± 10 cm s^{-1}, except for several cases at Station CM4, where discrepancies reach 20–30 cm s^{-1}. A markedly different situation is found in the layer shallower than 400 m depth at Station CM2, located closer to the coast. Here, measured velocities are generally higher than estimated values by approximately 20 cm s^{-1}. In particular, for the September 1994 section (Fig. 3 (c)), the difference reaches 80 cm s^{-1} at 300 m depth, associated with sharp velocity increase from 10 cm s^{-1} at 400 m depth to 140 cm s^{-1} at 300 m depth, corresponding to a strong vertical velocity shear of 1.3×10^{-2} s^{-1}, as measured by the moored-ADCP. These differences are likely due in part to the time required for both the density field and geostrophic velocity to adjust to abrupt changes in strong vertical velocity shear. Additionally, they may result from methodological differences; the AGVs represent averages over the distance between two hydrographic stations separated by 20 km, whereas the moored-ADCP velocities are point values at the middle of those stations. The estimated AGVs are generally consistent with upper-layer velocities measured by the towed-ADCP, although a direct comparison is not possible due to differences in observation dates.

The vertical section of the Eulerian-mean AGV (Fig. 7) was constructed from the eight AGV sections, providing a two-year mean, full-depth AGV section of the Kuroshio, for the first time, based on directly measured properties. This mean section represents the Kuroshio primarily during its nearshore path, except for one section at the beginning of the first offshore path period (May 1994), which exhibited only a weak countercurrent below 200 m depth near the coast. The main body of the Kuroshio was confined to the upper 1000 m, and the entire Kuroshio was virtually confined to the upper 1500 m. This mean flow is hereafter referred to as the

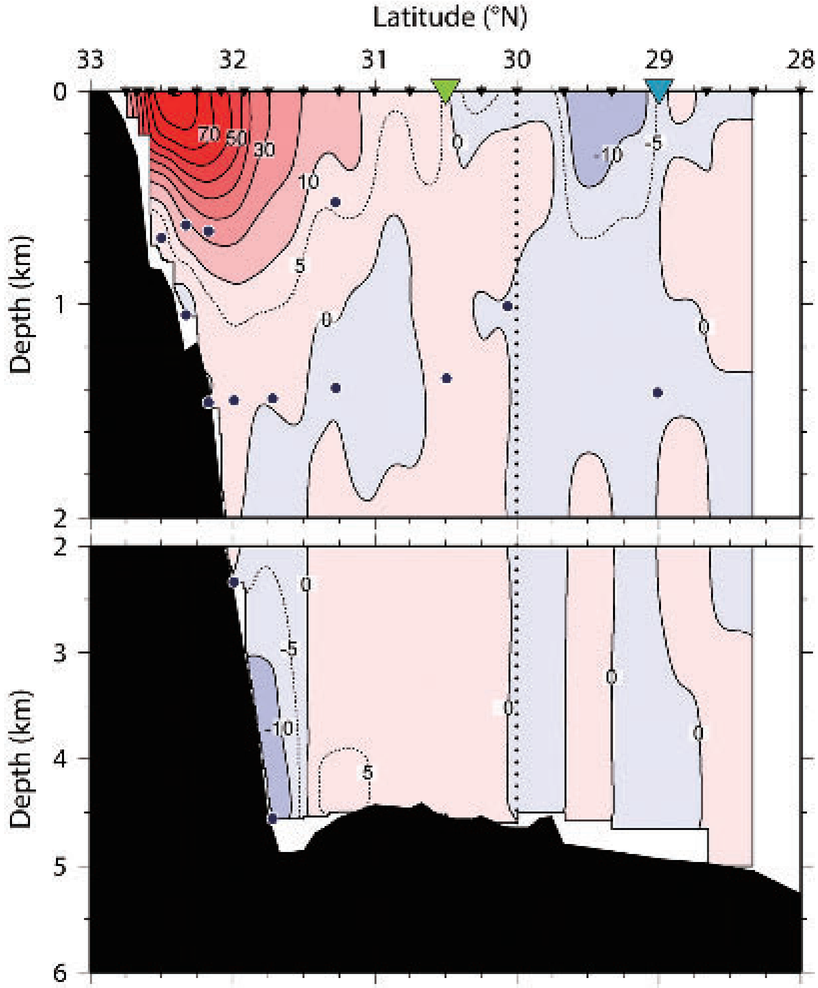

Fig. 7 Vertical section of the Eulerian-mean AGV (in cm s^{-1}) along the ASUKA line during 1994–1995. North of the dotted line at 30° N, eight AGV sections were averaged; south of this line, four sections were averaged. Triangles at the top denote locations of coordinated common hydrographic stations; the yellowish green triangle marks the inferred offshore edge of the mean Kuroshio, and the light blue triangle marks the inferred southern end of the mean Kuroshio recirculation. Dots denote mean locations of moored CMs providing velocities at reference levels or on the continental slope. From IMAWAKI et al. (2023).

mean Kuroshio. The maximum velocity (> 80 cm s^{-1}) was located at the sea-surface near the coast. Both vertical and horizontal velocity shears were stronger on the nearshore side than on the offshore side. The Kuroshio axis exhibited an offshore shift with increasing depth. These two features (i. e., velocity shear and offshore shift) are generally characteristic of mid-latitude western-boundary currents along the coast, as observed in the Kuroshio (e. g., KAWABE, 1985;

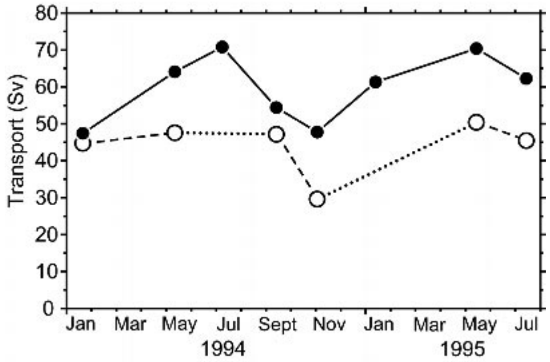

Fig. 8 Temporal series of total AGTs (absolute geostrophic transports; in Sv) of the Kuroshio (solid circles) and the throughflow Kuroshio (open circles) across the ASUKA section during 1994–1995. Adapted from IMAWAKI et al. (2023).

KANEKO et al., 1992; JOHNS et al., 2001), the Florida Current/Gulf Stream in the North Atlantic (e.g., HALKIN and ROSSBY, 1985; LEAMAN et al., 1989; JOHNS et al., 1995), and the Agulhas Current in the Indian Ocean (e.g., BRYDEN et al., 2005; BEAL et al., 2006; 2015).

BOOK et al. (2002a) derived a Eulerian-mean proxy AGV section along the ASUKA line for a five-month period (November 1993–April 1994) using IES and moored CM data, by applying the gravest empirical mode (GEM) method. The resulting flow field was essentially similar to the above-mentioned mean field in the upper 2000 m; the maximum velocity (> 90 cm s^{-1}) was located at the sea-surface near the coast, and the main body of the Kuroshio was mostly confined to the upper 1000 m. However, the deep flow structure near the continental slope, such as the deep westward flow described in Subsection 3.3, was not able to be described by their GEM method. They identified three smaller-scale meanders during the two-year observation period, in addition to three above-mentioned meanders, suggesting a four-month periodicity of Kuroshio meanders off Shikoku. This periodicity was further investigated by KASHIMA et al. (2009), who interpreted them as modulated periodic meanders having 110- or 150-day periods during 1993–2001. These variations were attributed to arrival of mesoscale eddies propagating westward from the ocean interior along 27–32° N latitudes.

3.2 Transport of the Kuroshio

Transport of the Kuroshio and the throughflow Kuroshio across the ASUKA section was estimated using multiple approaches (Table 1). From the eight full-depth AGV sections, the following transport values were estimated by IM23. The total AGT of the Kuroshio was estimated by integrating the positive AGV from the coast to the offshore edge of the Kuroshio, and from the sea-surface down to a maximum of 2000 dbar. This upper limit was imposed because contamination with deep eastward flows different from the Kuroshio, such as the eastward flow over the Nankai Trough (see the next subsection), should be minimized, and also because the Kuroshio was virtually confined to the upper 2000 m, as shown below. The total AGTs derived from the eight AGV sections provided a temporal series of Kuroshio transport estimates at relatively short intervals over a two-year period (solid circles in Fig. 8). These estimates varied substantially from 47 to 71 Sv, likely reflecting fluctuations induced by propagating mesoscale eddies as well as fluctuations of the throughflow Kuroshio and Warm Eddy off Shikoku. The mean AGT was estimated at 60 ± 9 Sv (mean ± standard deviation).

On the other hand, the total AGT of the mean Kuroshio (Fig. 7) was estimated at 47 Sv, corresponding to only 79% of the mean AGT of the instantaneous Kuroshio. This discrepancy arises because, in some cases, the instantaneous Kuroshio extended beyond the offshore edge of the

Table 1. Mean volume transports (mean ± standard deviation; in Sv) of the Kuroshio and the throughflow Kuroshio across the ASUKA (Affiliated Surveys of the Kuroshio off Cape Ashizuri) section estimated by various methods. See Section 1 for definitions and the listed sections/subsections for methodological details.

Data used	Kuroshio	throughflow Kuroshio	Duration (year)	Note	Reference	Section in the text
Total Transport						
CTD & CM	60±9	44±7	2 (1994–1995)	AGTs based on eight full-depth sections	Imawaki et al. (2023)	3.2
IES & CM	65±20	–	2 (1993–1995)	Proxy AGTs, using GEM method	Book et al. (2002a)	3.2
Altimetry	61±16	35±8	31 (1993–2024)	Proxy GTs, using an empirical relationship	Uchida (2025) & Imawaki et al. (2025)	5
Transport in the upper 1000 m						
CTD & CM	56±8	–	2 (1994–1995)	AGTs based on eight full-depth sections	Imawaki et al. (2023)	3.2
CTD/XBT & CM	54±13	–	2 (1993–1995)	AGTs based on 25 sections	Imawaki et al. (2001)	3.2
IES	45±10	–	5 (1994–1997, 2001)	Proxy GTs referred to 1000 dbar, using GEM method	Kakinoki et al. (2008b)	4
Altimetry	57±11	42±9	7 (1992–1999)	Proxy AGTs, using an empirical relationship	Imawaki et al. (2001)	5

AGT: absolute geostrophic transport; CM: current-meter; CTD: conductivity-temperature-depth recorder; GEM: gravest empirical mode; GT: geostrophic transport; IES: inverted echo sounder; XBT: expendable bathy-thermograph mean Kuroshio, while in other cases, the instantaneous Kuroshio recirculation intruded into the region of the mean Kuroshio.

Vertical profiles of AGT per unit depth for the Kuroshio showed that the transport was predominantly located in the upper 1000 m (Fig. 4 of IM23). AGTs within this upper 1000 m varied from 44 to 68 Sv, with a mean of 56 ± 8 Sv. These values represented 90–97% of the total AGT, with a mean of 93 ± 3%. For the mean Kuroshio, transport was even more concentrated in the upper 1000 m, which accounted for 97% of the total transport. The profiles also showed that AGTs between 1500 and 2000 m depth were negligibly small, confirming that the transport was virtually confined to the upper 2000 m. The trivially small transport in the deep layer is likely attributable to the bottom topography around the Kuroshio. The Tokara Strait is shallower than 690 m (NAKAMURA, 2017), and the portion of the Izu-Ogasawara Ridge over which the Kuroshio usually flows is shallower than approximately 1500 m (OTSUKA, 1985), although the Ryukyu Current region is relatively deep.

The AGT of the Kuroshio recirculation (positive denotes westward) was estimated for the upper 2000 m using a similar approach, with the exception that net AGT between hydrographic stations was integrated, instead of positive AGV. This modification was necessary because of the complex velocity field due to overlapping mesoscale eddies. Estimated AGTs of the recirculation varied from 3 to 20 Sv, with a mean of 14 ± 7 Sv. The AGTs of the throughflow Kuroshio were then estimated by subtracting the AGTs of the Kuroshio recirculation from the AGTs of the Kuroshio. Estimated AGTs varied from 30 to 50 Sv, with a mean of 44 ± 7 Sv (open circles in Fig. 8).

For comparison, ordinary GTs of the Kuroshio, referred to 2000 dbar, were similarly estimated from the full-depth sections. The deviations from the corresponding AGTs were relatively small, with a mean of 2 ± 4 Sv. Positive deviations occurred when the upper boundary of the deep westward flow over the Nankai Trough (see the next subsection) was shallower than 2000 m. These results suggested that GT referred to and calculated above 2000 dbar can be used for monitoring transport in cases where velocities at the reference level are not available (IM23).

BOOK et al. (2002a) derived a proxy time series of daily AGT of the Kuroshio from IES and moored CM data for the two-year observation period, by applying the GEM method and integrating velocity over the contiguous region of eastward AGV encompassing the Kuroshio. The resulting proxy AGTs ranged from 25 to 139 Sv, with a mean of 65 ± 20 Sv, which is slightly larger than the mean AGT of the Kuroshio (60 Sv) estimated from the eight full-depth CTD sections by IM23 (Table 1).

IMAWAKI et al. (2001) estimated the AGT of the Kuroshio in the upper 1000 m for 25 selected high-quality hydrographic sections from 1993 to 1995, referred to velocities measured at the 700 m level. Their analysis utilized plentiful XBT data in addition to CTD data. Although the XBTs provided only temperature profiles down to approximately 800 m depth, geostrophic velocities down to 1000 m depth were calculated using very tight temperature-salinity relationships and skillful extrapolation of steric height (UCHIDA and IMAWAKI, 2008). Note that most of Kuroshio transport (93% on average) is located in the upper 1000 m, as shown above. The AGT was estimated as the net transport between the coast and offshore edge of the Kuroshio.

Estimated AGTs ranged from 27 to 85 Sv, with a mean of 54 ± 13 Sv, which is slightly smaller than the mean AGT (56 Sv) in the upper 1000 m estimated from the eight full-depth sections discussed above. A scatter plot of AGTs in the upper 1000 m versus SSDT differences across the Kuroshio (Fig. 9 (a)) revealed a strong linear relationship, with a CC of 0.90 and small standard deviation of 5.6 Sv about the regression line (IMAWAKI et al., 2001). This strong correlation can be explained by examining vertical profiles of transport per unit depth (Fig. 9 (b)). Although the original profiles exhibited considerable variability, normalization by the sea-surface transport yielded nearly identical shapes across different observations. This result indicated that the total transport was approximately proportional to the sea-surface transport, which is proportional to the SSDT difference across the Kuroshio, under the assumption of geostrophy. This linear relationship had previously been identified for the Kuroshio south of Japan (NITANI, 1975) and the Florida Current (e.g., MAUL et al., 1985), as discussed in more detail in the Appendix. This empirical relationship provided a practical method for long-term monitoring of volume transport using satellite altimetry data. The resulting time series of Kuroshio transport is shown in Section 5.

One of the main aims of the WOCE was to estimate oceanic heat transport (SIEDLER et al., 2001). To evaluate heat transport at midlatitudes in the North Pacific, AGV and hydrographic data from the Kuroshio region, obtained during the ASUKA intensive observation, were combined with data from the WOCE Hydrographic Program P2 section along 30° N (BRYDEN and IMAWAKI, 2001). This trans-Pacific hydrographic section was carried out in 1993–1994 by three Japanese vessels: the survey vessel *Shoyo*, the fisheries research vessel *Kaiyo-maru*, and the training vessel *Bosei-maru* (e.g., YOU et al., 2003). The westernmost part of the P2 section, occupied in January 1994, was connected to the full-depth Kuroshio section occupied nearly

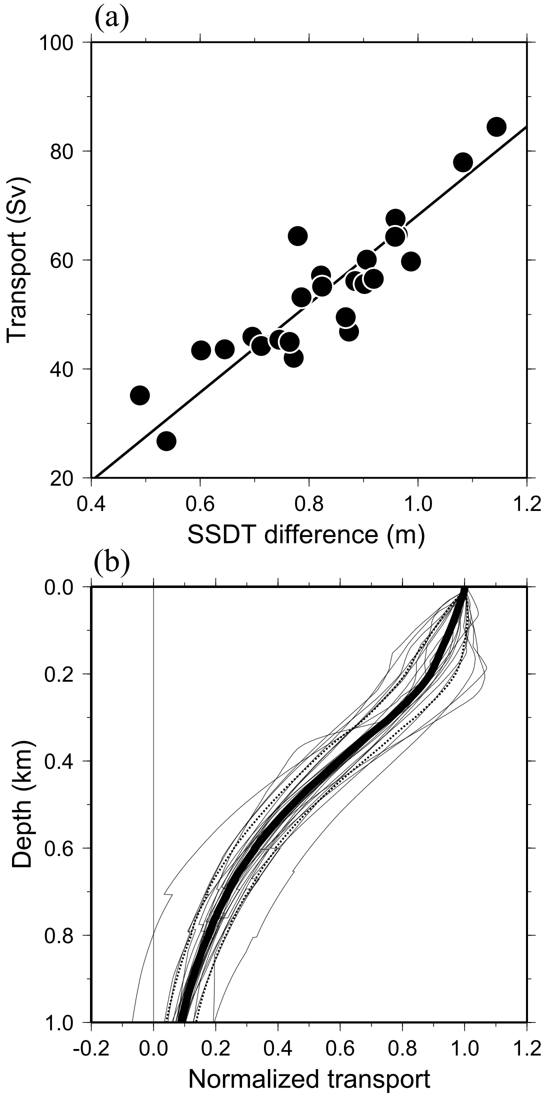

Fig. 9 AGT of the Kuroshio in the upper 1000 m during 1993–1995. (a) Scatter plot of AGTs (in Sv) versus SSDT (sea-surface dynamic topography) differences (in m) across the Kuroshio. The solid line denotes the regression line. (b) Vertical profiles of AGT per unit depth, normalized by the sea-surface AGT. The mean profile (thick line) and its standard deviation (dotted lines) are shown as well as 25 instantaneous profiles (thin lines). From IMAWAKI et al. (2001).

simultaneously, instead of the mean Kuroshio section. This decision was made because a very strong cyclonic mesoscale eddy was located precisely at the junction point, and hence its influence on the two sections should cancel out as much as possible. The estimated net northward heat transport across 30° N was 0.62×10^{15} W, corresponding to approximately 40% of the global oceanic northward heat transport ($1.6 \pm 0.4 \times 10^{15}$ W) at 24° N, as estimated by MACDONALD and BARINGER (2013). Connecting a one-time transoceanic section with a western-boundary current section remains a complex methodological challenge.

3.3 Flows under the Kuroshio

The time series of daily current vectors at the 700 m level at Station CM2 (Fig. 6 (a)) exhibited an anomalous pattern, distinctly different from the typical Kuroshio flow (UMATANI et al., 2001). Specifically, the vectors were directed primarily to the southwest, with occasional northeast, and fluctuated in an almost unidirectional manner. The two-year mean velocity vector was oriented west-southwest, with a magnitude of 7 cm s^{-1} (Fig. 5). This flow was clearly influenced by the bottom topography, because the CM was moored only 130 m above the bottom at a depth of 820 m and the observed flow direction corresponded closely with contours of the bottom topography. Note that this flow was located beneath the strong upper-layer currents of the Kuroshio. Flow speed increased when the Kuroshio took the offshore path and thus coastal countercurrents were present in the upper-layer (Fig. 6 (a)). The two-year mean velocities measured by CMs near the bottom at Stations CM3 and CM4 were −7 and −11 cm s^{-1}, respectively (KAKINOKI et al., 2008a). This steady, topographically controlled countercurrent extended along the continental slope down to a depth of 2000 m beneath the Kuroshio (Fig. 2 of UMATANI et al., 2001).

The record from the CM near the bottom at Station CM6 (Fig. 6 (b)), moored at the base of the continental slope, also exhibited atypical behavior (UMATANI et al., 2001), with the flow pattern differing markedly from that of the Kuroshio at 700 m depth at the same station (see Fig. 6 (a)). The current was directed consistently toward the west-southwest, parallel to contours of the bottom topography, and fluctuated only in speed. The maximum speed was 30 cm s^{-1}, and the speed of a 1.6-year mean vector was 15 cm s^{-1}. At 3000 m depth at the same station, the flow pattern was similar but weaker; the speed of a one-year mean vector was 8 cm s^{-1}. In contrast, the flow at 1500 m depth was weak and did not resemble the near-bottom flow. In summary, this bottom-intensifying flow weakened with decreasing depth and dissipated between 1500 and 3000 m depth.

This west-southwestward flow was clearly identified in the full-depth AGV sections (IM23) and in the mean AGV section (Fig. 7), where westward flow was observed along the lower continental slope, from approximately 2000 m depth to the bottom at about 4500 m depth, between 32° and 31° 30'N. Its velocity exceeded 10 cm s^{-1} and intensified with depth. On the offshore side, a distinct eastward flow was observed from approximately 2000 m depth down to the bottom between 31° 30' and 31° N. The flow also intensified with depth. This pair of deep westward and eastward flows was suggested to constitute a localized, anticlockwise, abyssal circulation dynamically trapped by the Nankai Trough (see Fig. 1 for location). Part of the westward flow was consistent with the basin-wide abyssal circulation in the Shikoku Basin previously suggested by FUKASAWA et al. (1987; 1995). The CC of transport between the westward and eastward flows was −0.50, which was fairly high given that the westward flow appeared to contribute to the basin-wide circulation other than the localized circulation over the Trough. The AGT of the main portion of the deep westward flow over the Trough was estimated at −10 ± 3 Sv, on average, and that of the eastward flow at 8 ± 4 Sv (IM23). These deep flows were likely independent of the Kuroshio locally, as indicated by low CCs of transport between these flows and the Kuroshio.

4. After the intensive observation

Two IESs at Stations IES1 (32° 35'N) and IES7 (31° N) were maintained continuously following the ASUKA intensive observation. Proxy GT (referred to and calculated above 1000 dbar) between these two stations was estimated using the GEM method (Kakinoki et al., 2008b). The proxy GTs derived from IES data showed excellent agreement with *in situ* GTs between the same stations. Station IES7 was located near the average offshore edge of the Kuroshio (30° 50'N), and thus estimated transports roughly represented Kuroshio transport. The estimated GTs ranged from 18 to 77 Sv, with a five-year mean of 45 ± 10 Sv. This value is approximately 20% smaller than the mean AGT of the Kuroshio in the upper 1000 m (54–56 Sv) during the intensive observation period (Table 1). The discrepancy is primarily attributable to the relatively shallow reference level of 1000 dbar used in the proxy GT calculation, which results in a loss of 18% of AGT on average (Fig. 9 (b)).

Hydrographic surveys along the ASUKA line continued through 2010, conducted by the Japan Meteorological Agency, several universities, the Fisheries Agency, the former Maritime Safety Agency, and the Japan Agency for Marine-Earth Science and Technology. The Japan Meteorological Agency, in particular, carried out surveys three to six times each year during the period 1993–2009. In addition, the northern part was occupied by the research vessel *Melville* in 2004 as a revisit of the WOCE Hydrographic Program P2. As a result, a total of 163 hydrographic sections were obtained, yielding an excellent mean section of geostrophic velocity as shown in the next section. The metadata for surveys conducted through May 2008 are summarized by Uchida et al. (2008).

Using the hydrographic data collected along the ASUKA line, subsequent studies were carried out as follows, although most are not considered as part of the ASUKA program. Zhu et al. (2006) compared the AGT of the Kuroshio south of Japan with those of the Kuroshio in the East China Sea and the Ryukyu Current. Guo et al. (2013) investigated nutrient transport by the Kuroshio from the East China Sea to the region south of Japan. Qiu and Chen (2021) described a cyclonic trigger meander and the Warm Eddy off Shikoku as key processes contributing to the occurrence of the large meander. Nagano et al. (2010) compared AGTs of the Kuroshio and the throughflow Kuroshio between large meander and non-large meander states. In addition to these hydrographic surveys, six pressure-recording IESs (PIESs) were deployed along the ASUKA line during 2004–2006 to investigate bottom pressure change associated with the large meander (Nagano et al., 2018). These PIES data were also used to derive a proxy time series of GT for the throughflow Kuroshio by combining satellite altimetry data (Nagano et al., 2013). Furthermore, Uchida and Imawaki (2008) examined the sea-level trend south of Japan from 1992 to 2006 using these hydrographic data in combination with satellite altimetry data.

5. Time series of transport

Using the linear relationship between the

AGT of the Kuroshio and the SSDT difference across the Kuroshio, as described in Subsection 3.2, a proxy time series of Kuroshio transport was derived from TOPEX/Poseidon altimetry data as follows (IMAWAKI et al., 2001). The unknown mean SSDT for the period 1993–1995 was estimated by subtracting the altimetric anomaly from the *in situ* SSDT obtained simultaneously. The *in situ* SSDT was calculated by integrating sea-surface AGVs, referred to the tide gauge data. The AGVs were referred to velocities measured at the 700 m level.

Using the altimetrically derived total SSDT together with the previously established linear relationship, a proxy time series of AGT for the Kuroshio in the upper 1000 m was derived for seven years (1992–1999) at ten-day intervals. The altimetrically derived transports showed excellent agreement with *in situ* AGT estimates of the Kuroshio. The seven-year mean AGT of the Kuroshio was estimated at 57 ± 11 Sv, slightly larger than the two-year mean *in situ* AGT (54–56 Sv) in the upper 1000 m during the intensive observation period (Table 1). A proxy time series of AGT for the Kuroshio recirculation was also derived using a similar method, but the southern end of the recirculation was fixed at 26° N, which was close to its climatological-mean position (HASUNUMA and YOSHIDA, 1978). By subtracting the AGT of the Kuroshio recirculation from the AGT of the Kuroshio, the AGT of the throughflow Kuroshio was estimated at 42 ± 9 Sv, on average. This value was slightly smaller than the two-year mean *in situ* AGT of 44 Sv (Table 1).

As an extension of IMAWAKI et al. (2001), three-decade-long proxy time series of GT for the Kuroshio and the throughflow Kuroshio were derived as follows. Vertical sections of mean potential temperature and salinity were obtained from 145 hydrographic surveys along the ASUKA line for 1992–2006 (UCHIDA and IMAWAKI, 2008). Based on these mean sections, a geostrophic velocity section referred to 1800 dbar was calculated (UCHIDA, 2025). Here, the reference level of 1800 dbar was selected to utilize hydrographic sections slightly shallower than the 2000 dbar recommended by IM23. Subsequently, net GTs above 1800 dbar were estimated between the nearshore-most hydrographic station (AS1) and other stations, and compared with SSDT differences between the corresponding stations. As shown in Fig. 10, the comparison for stations in the offshore-side Kuroshio and Kuroshio recirculation regions revealed an extremely strong linear relationship, with a CC of 0.99 (UCHIDA, 2025). This beautiful association resulted from eliminating effect of mesoscale eddies almost perfectly by averaging a great number of hydrographic sections. While vertical profiles of transport in Fig. 9 show that the vertically integrated transport is proportional to the sea-surface transport for the whole Kuroshio, the regression line in Fig. 10 furthermore indicates that the integrated transport is proportional to the sea-surface transport for each pair of hydrographic stations with a constant ratio, even for negative transport. It suggests that the offshore-side Kuroshio and its recirculation have a common vertical velocity structure with opposite directions, which is natural because those two make up the Warm Eddy off Shikoku.

Using this linear relationship and altimetrically derived total SSDT (Fig. 11 (b)) estimated by the same method described above, time series of stream function for net GTs integrated from the coast to offshore locations along the ASUKA line were generated. The time series spanned the most recent three decades with ten-day intervals (UCHIDA, 2025).

From these time series, a proxy time series of GT for the Kuroshio (red dots and line in Fig. 11

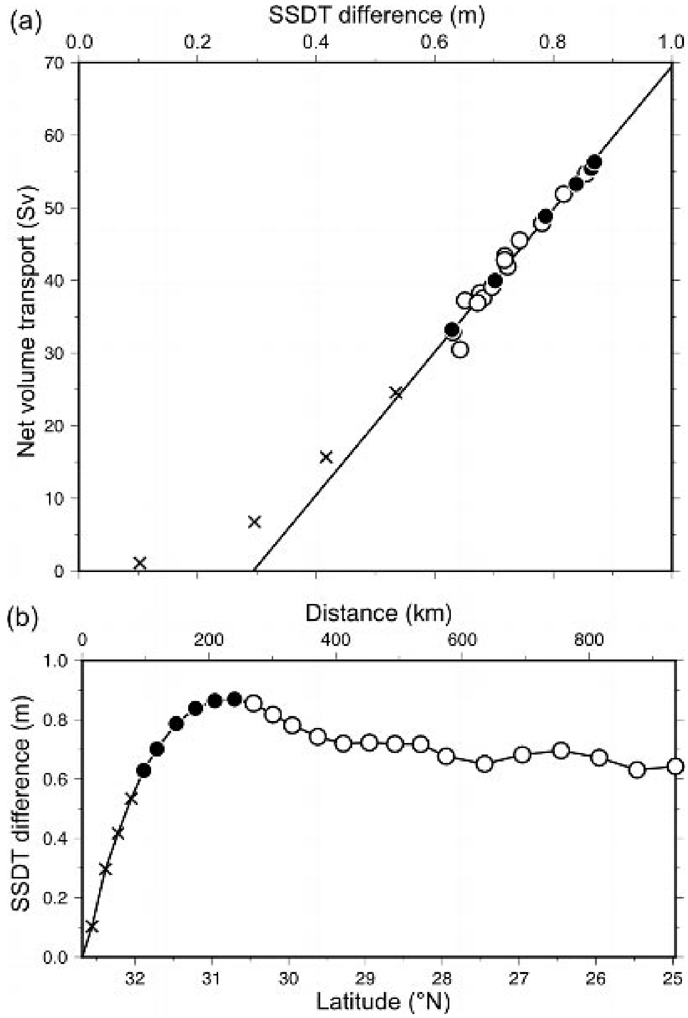

Fig. 10 Net volume transport and SSDT difference along the ASUKA line, estimated from the mean geostrophic velocity section (referred to 1800 dbar) averaged over the period 1992–2006. (a) Scatter plot of net volume transports (in Sv) versus SSDT differences (in m), both between the nearshore-most hydrographic station (AS1) and other stations along the ASUKA line. Solid and open circles show values at stations in the offshore-side Kuroshio region (AS6–AS11) and in the Kuroshio recirculation and further offshore regions, respectively. Crosses show values at four stations in the nearshore-side Kuroshio region (AS2–AS5). The solid line denotes the regression line fitted to data points shown by the solid and open circles, applicable only to the offshore regions; the four nearshore stations were excluded because water depth was shallow and hence the relationship was different. The correlation coefficient was 0.99. (b) Profile of the SSDT difference along the ASUKA line. Adapted from Uchida (2025).

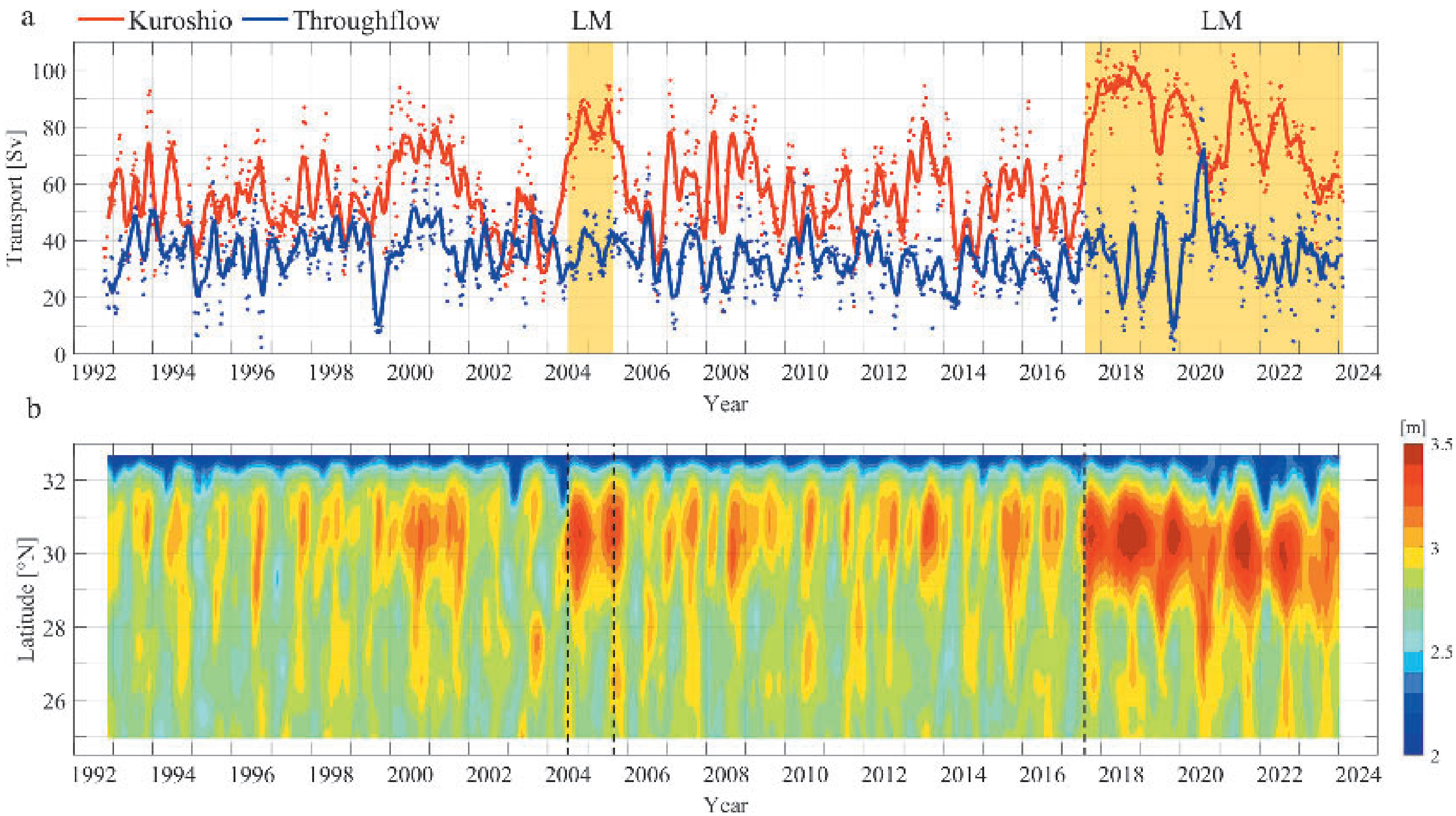

Fig. 11 Proxy time series of GT across the ASUKA section and SSDT along the ASUKA line, during 1992–2024, estimated from combined satellite altimetry and hydrography data. In (a), red and blue dots represent transport (in Sv) for the Kuroshio and the throughflow Kuroshio, respectively (see text for definitions), every ten days . Red and blue lines denote their 90-day running means. Ocher-shaded intervals mark large meander periods. (b) Latitude–time plot of SSDT (in m), after applying a 90-day running-mean filter. Vertical dashed lines denote the start and end of the large meander periods. From Imawaki et al. (2025).

(a)) was derived (IMAWAKI et al., 2025). The estimated GTs corresponded well with *in situ* AGTs during the intensive observation period. The mean GT during 1992–1999 was estimated at 54 Sv, which was slightly smaller than the mean altimetrically derived AGT (57 Sv) in the upper 1000 m for the same period (Table 1). The 31-year mean transport of the Kuroshio (for 1993–2023) was estimated at 61 ± 16 Sv. Fluctuations of Kuroshio transport were primarily associated with the Warm Eddy off Shikoku and did not significantly reflect fluctuations of the western-boundary transport expected to compensate for interior Sverdrup transport over a flat bottom (WBST), which was estimated by integrating wind-stress curl over the North Pacific subtropical gyre.

A proxy time series of GT for the throughflow Kuroshio (blue dots and line in Fig. 11 (a)) was also derived using a similar method (IMAWAKI et al., 2025). In this case, the southern end of the Kuroshio recirculation was fixed at 27° 30'N, which was close to its mean position inferred from the average SSDT profile along the ASUKA line for 1993–2023. However, agreement with *in situ* AGT estimates during the intensive observation period was limited. The discrepancy was likely due to both contamination from mesoscale eddies and incomplete coverage of the Kuroshio recirculation in some sections in IM23. The mean altimetrically derived GT of the throughflow Kuroshio for 1992–1999 was estimated at 36 Sv, which was smaller than the mean altimetrically derived AGT (42 Sv) in the upper 1000 m for the same period (Table 1). The 31-year mean of annual-mean transport of the throughflow Kuroshio was estimated at 35 ± 5 Sv. This is considerably smaller than the corresponding mean of WBST of 45 ± 4 Sv. On an interannual scale, fluctuations of throughflow transport were found to correspond with those of WBST, with a lag of approximately five years. Interestingly, the mean throughflow transport during large meander periods was nearly identical to that during non-large meander periods.

6. Discussion

The ASUKA intensive observation provided, for the first time, temporal series of full-depth AGV sections and total AGTs of the Kuroshio off Shikoku at two- to four-month intervals over a two-year period, based on a dense CM mooring array and repeated hydrographic surveys. The estimated AGTs were similar to the AGT in 1971 of 57 Sv referred to moored CM data (TAFT, 1978), but smaller than that in 1965 of 84 Sv referred to neutrally-buoyant float data (WORTHINGTON and KAWAI, 1972).

The Kuroshio east of Taiwan, marking the entrance to the East China Sea, was observed during the WOCE (1994–1996) using a moored-instrument array (designated the WOCE PCM1 array), which included CMs, ADCPs, and CTDs. The 20-month mean volume transport of the Kuroshio was estimated at 22 ± 3 Sv (JOHNS et al., 2001; LEE et al., 2001). Subsequently, the transport of the Kuroshio through the Tokara Strait was estimated at 26 ± 3 Sv on average for the period 2003–2012, based on ferry-mounted ADCP data (LIU et al., 2019). These findings indicate that the transport of the Kuroshio through the East China Sea is approximately half of the transport of the throughflow Kuroshio off Shikoku estimated from the ASUKA data. The difference between these two transport estimates is primarily attributed to the contribution of the Ryukyu Current (Fig. 1), which flows northeastward along the Ryukyu Islands and merges with the Kuroshio exiting the East China Sea (east of the Tokara Strait), as described by ICHIKAWA et al. (2004), ZHU et al. (2006), ANDRES et al. (2008), THOPPIL et al. (2016), and ZHAO et al. (2020).

As part of the WOCE program, the Kuroshio southeast of near Cape Inubo (east of the Izu-Ogasawara Ridge) was observed in 1993 during a hydrographic survey along the 149° E meridian (designated the WOCE Hydrographic Program P10). The total AGT of the Kuroshio was estimated at 143 Sv, referred to one-time lowered-ADCP data (WIJFFELS et al., 1998). This exceptionally large transport was mostly due to a strong local recirculation south of the Kuroshio (CHEN et al., 2007). The transport of the throughflow Kuroshio was estimated at approximately 50 Sv by QIU (2002), which was comparable to some larger-end estimates obtained during the ASUKA intensive observation period.

The mean annual variation of Kuroshio transport, estimated from IES data for the period 1994–1997, showed an almost sinusoidal seasonal cycle with a maximum in September and a minimum in March, and a relatively small amplitude of 8 Sv (KAKINOKI et al., 2008b). In contrast, the mean annual cycles of transport for both the Kuroshio and the throughflow Kuroshio, estimated from the three-decade-long time series, exhibited two maxima and two minima, with peaks in July and ranges of 8–9 Sv (IMAWAKI et al., 2025); it should be noted that the estimated annual cycles are to some extent contaminated by possible seasonality of the used empirical relationship between transport and SSDT difference. Conversely, the WBST showed a simple seasonal cycle, with a maximum in December/January and a minimum in September/October, and a much larger amplitude of 47 Sv (IMAWAKI et al., 2025).

The attenuation of the annual cycle of observed transport relative to WBST was attributed to the influence of the Izu-Ogasawara Ridge, which acts as a barrier to the westward-propagating seasonal barotropic signals from the ocean interior, converting them into baroclinic signals (e.g., ISOBE and IMAWAKI, 2001). Regarding the observed delay of the western-boundary transport, a summer maximum transport was reproduced in an idealized two-layer planetary geostrophic model incorporating variable bottom topography and forced by sea-surface heat flux as well as wind-stress (SAKAMOTO, 2005). The summer maximum was also shown in the upper-layer transport induced by seasonal wind variation over the Kuroshio in the East China Sea (ZHANG et al., 2021), suggesting that local processes may contribute considerably to the seasonal cycle. Further studies are needed to fully understand the seasonal variability of Kuroshio and throughflow Kuroshio transport.

Transport of the throughflow Kuroshio is typically estimated indirectly by subtracting the transport of the Kuroshio recirculation from the transport of the Kuroshio. Direct estimation is possible if the throughflow Kuroshio and the Warm Eddy off Shikoku can be clearly separated. To distinguish these two components, the use of potential vorticity of the North Pacific Subtropical Mode Water (KANEKO et al., 2001) and water-type analysis based on spiciness (FLAMENT, 2002; NAGANO et al., 2009; 2010) has been suggested. Note that these approaches require densely spaced hydrographic stations in the Kuroshio region and a well-defined boundary, because the boundary is located in the middle of large transport. An alternative method for direct estimation is construction of net transport from the coastline, as reported by IMAWAKI et al. (2025).

The Gulf Stream between the Florida Strait and Cape Hatteras is the counterpart to the Kuroshio south of Japan (WORTHINGTON and KAWAI, 1972). HEIDERICH and TODD (2020) summarized volume transport of the Gulf Stream in the upper 1000 m, primarily based on autonomous underwater glider data obtained during 2004–2020.

The mean transport in the central portion of that region was estimated at 38–44 Sv, which is smaller than the Kuroshio transport (54–56 Sv) in the upper 1000 m during the ASUKA intensive observation period. The vertical profile and magnitude of transport per unit depth are broadly similar to those of the Kuroshio (Fig. 4 of IM23). In both flows, transport decreases monotonically from the sea-surface to 800 m depth. One noted difference is a slight increase in Gulf Stream transport between 800 to 1000 m depth. General features of the western-boundary currents in the five major oceans were briefly reviewed by IMAWAKI et al. (2013).

Numerous studies have examined the relationship between volume transport and the SSDT difference across major ocean currents worldwide, as outlined in detail in the Appendix. Most of these studies have demonstrated that the linear relationship holds, making it possible to derive proxy time series of transport from satellite altimetry data. For example, the linear relationship has been identified for the Kuroshio at the Tokara Strait (LIU et al., 2021), in the East China Sea (ANDRES et al., 2008), and east of Taiwan (YANG et al., 2001), as well as south of Japan (NITANI, 1975; IMAWAKI et al., 2001). Similar relationships have also been observed in other midlatitude western-boundary currents, including the Oyashio in the northwestern North Pacific (ITO et al., 2004), the Gulf Stream southeast of Cape Cod (BREARLEY, 2010), the Brazil Current in the South Atlantic (GOES et al., 2019), and the Agulhas Current (BEAL and ELIPOT, 2016).

In contrast to most western-boundary currents, the East Australian Current in the South Pacific is characterized by relatively active mesoscale variability, and the linear relationship has not been confirmed (e.g., RIDGWAY et al., 2008; ZILBERMAN et al., 2018). For the Antarctic Circumpolar Current across the 140° E meridian, RINTOUL et al. (2002) reported a very tight relationship between net GT integrated from the southern end to a given latitude and the SSDT at that latitude. In contrast, for that Current in the Drake Passage, variability of narrow frontal jets required the use of a look-up table for the vertical profile of velocity as a function of latitude and sea-surface velocity, to derive a time series of transport (KOENIG et al., 2014). In the case of the Indonesian Throughflow, flows were different above and below 150 m depth, and a time-lagged partial regression model was required to estimate transport (SPRINTALL and RÉVELARD, 2014).

With respect to the deep westward flow over the Nankai Trough, a southwestward flow on the lower continental slope was first identified in 1965, with an estimated transport of −6 Sv (WORTHINGTON and KAWAI, 1972). A similar southwestward flow having a transport of −4 Sv was observed on the slope in 1971 (TAFT, 1978). FUKASAWA et al. (1987) reported a very steady west-southwestward flow, exactly aligned with contours of the local bottom topography, based on moored CM data obtained over the slope in 1984–1985. The ASUKA data further confirmed the presence of a west-southwestward flow over the slope, with a speed of 1.6-year vectorial-mean of 15 cm s^{-1} (UMATANI et al., 2001) and an associated mean transport of −10 Sv (IM23). These deep west-southwestward flows likely form part of the basin-wide anticlockwise abyssal circulation in the Shikoku Basin, originally suggested by FUKASAWA et al. (1987; 1995).

The ASUKA data also revealed an eastward flow on the offshore side of this west-southwestward flow, similarly intensifying toward the bottom. This pair of opposing abyssal flows was interpreted as a manifestation of a local anticlockwise abyssal circulation trapped dynamically by the Nankai Trough (IM23). A similar pair of deep counterflows had been observed over the Izu-Ogasawara Trench, consisting of a southward flow on the western slope and northward flow on the eastern slope (FUJIO et al., 2000).

7. Summary

The ASUKA Group conducted intensive observation of the Kuroshio and its recirculation off Shikoku in 1993–1995, primarily to estimate volume transport of the Kuroshio and the throughflow Kuroshio. During this period, the Kuroshio took the non-large meander path. The observation was performed by moored and towed instruments, as well as frequently repeated hydrographic surveys. The observation line was oriented almost perpendicular to the typical path of the Kuroshio off Cape Ashizuri and aligned with the subsatellite track of the TOPEX/Poseidon altimeter. Over the two-year observation period, nine moorings equipped with 33 CMs and two ADCPs, and ten IESs were deployed. A total of 42 hydrographic sections were obtained for the upper 1000 m in the Kuroshio region, including eight full-depth CTD sections. In addition, towed-ADCP measurements were conducted on 12 occasions. The following is a summary of the major findings obtained from the ASUKA dataset and its combination with satellite altimetry data.

The Kuroshio took either a nearshore or offshore path during the observation period. During the nearshore path, a very strong vertical velocity shear, reaching $1.5 \times 10^{-2}\ s^{-1}$, was observed in the upper-layer of the Kuroshio near the coast. In contrast, during the offshore path, a very weak velocity shear of $0.04 \times 10^{-2}\ s^{-1}$ was observed in the upper-layer of the coastal countercurrent.

Geostrophic balance was confirmed to hold very well in both the intermediate layer (700–1500 m depth) and the deep layer (1500–3000 m depth), based on direct comparisons of vertical difference between geostrophic velocity and measured velocity. The strongest statistical agreement was obtained when measured velocities were averaged over several days.

Eight full-depth sections of AGV, referred to velocities measured at mid-depths, were obtained from CM moorings and hydrographic surveys. The total AGT of the Kuroshio was estimated by integrating eastward AGV from the coast to its offshore edge, and from the sea-surface to 2000 dbar at deepest. These AGT estimates, obtained at relatively short intervals over the two years, varied from 47 to 71 Sv, with a mean of 60 Sv. Vertical profiles of AGT per unit depth revealed that the majority of transport was concentrated in the upper 1000 m. There AGTs varied from 44 to 68 Sv, with a mean of 56 Sv, corresponding to 93% of the mean total AGT.

The Eulerian-mean AGV section was derived from the series of eight full-depth AGV sections. This represented the first two-year mean, full-depth AGV section of the Kuroshio based on directly measured properties. The main body of the mean Kuroshio was confined to the upper 1000 m, and the entire flow was virtually confined to the upper 1500 m. Both vertical and horizontal velocity shear were stronger on the nearshore side than on the offshore side. The Kuroshio axis at a given depth shifted offshore with increasing depth. The AGT of the Eulerian-mean Kuroshio was estimated at 47 Sv, corresponding to 79% of the mean AGT of the instantaneous Kuroshio.

AGTs of the Kuroshio recirculation were estimated using a similar method. They varied from 3 to 20 Sv, with a mean of 14 Sv. AGTs of the throughflow Kuroshio were estimated by subtracting the recirculation transports from the

Kuroshio transports. They varied from 30 to 50 Sv, with a mean of 44 Sv.

For comparison, conventional GTs of the Kuroshio, referred to and calculated above 2000 dbar, were also estimated from the full-depth CTD sections. Deviations from the corresponding AGTs were relatively small. Therefore, GT referred to and calculated above 2000 dbar was recommended for monitoring transport of the Kuroshio when velocities at reference levels are not available.

AGTs of the Kuroshio in the upper 1000 m were strongly correlated with SSDT differences across the Kuroshio. This linear empirical relationship provided a practical basis for long-term monitoring of volume transport using satellite altimetry data. Indeed, using this relationship and TOPEX/Poseidon altimetry data, a proxy time series of AGT for the Kuroshio was derived for the period 1992–1999. Further, an extremely strong linear relationship was identified between net GTs integrated from the coast to hydrographic stations in the offshore-side Kuroshio and Kuroshio recirculation regions, and SSDT differences over the same horizontal ranges. Based on this linear regression and altimetric SSDT data, a proxy time series of GT for the Kuroshio was derived for three decades (1992–2024) at ten-day intervals. The mean transport was estimated at 61 Sv. Fluctuations of Kuroshio transport were primarily caused by the Warm Eddy off Shikoku and did not significantly reflect fluctuations of WBST.

A similar approach was used to derive a proxy time series of GT for the throughflow Kuroshio for the three decades. The mean transport was estimated at 35 Sv, which was considerably smaller than the climatological-mean WBST (45 Sv). On interannual timescales, throughflow transport closely reflected WBST variability, with a lag of approximately five years. The mean throughflow transport was nearly identical during large meander and non-large meander periods.

Numerous studies have examined the relationship between volume transport and SSDT difference for major ocean currents worldwide. For most mid-latitude western-boundary currents, the linear relationship holds and can be used to derive a proxy time series of volume transport from satellite altimetry data.

Beneath the Kuroshio, a pair of stable westward and eastward flows, both intensifying toward the bottom, was observed over the Nankai Trough. This pair of opposing flows suggested the presence of a localized, anticlockwise, abyssal circulation dynamically trapped by the Trough. A portion of the westward flow also appeared to contribute to the basin-wide abyssal circulation in the Shikoku Basin. The AGT of the principal westward flow was estimated at −10 Sv, on average, and that of the eastward flow at 8 Sv.

Appendix: Relationships between volume transport and SSDT

The following are selected studies examining the relationship between volume transport and SSDT for various currents worldwide, excluding the Kuroshio off Shikoku. In most cases, the identified relationships were used to derive proxy time series of volume transport from satellite altimetry data. These studies are summarized in Table A1.

In the Oyashio region of the northwestern North Pacific, a strong linear relationship was observed with a CC of 0.93, based on 12 comparisons between GTs (referred to 3000 dbar) and SSDT differences across the same horizontal ranges. The GTs were derived from CTD sections southeast of Hokkaido, aligned with a TOPEX/Poseidon subsatellite track, while the SSDT differences were estimated from satellite

Table A1. Summary of observed linear relationships between volume transports and SSDT (sea-surface dynamic topography) differences across ocean currents, and their application to proxy time series of transport (positive denotes northward or eastward). See the Appendix for details.

Current	Linear relationship				Proxy time series			Reference
	Transport dealt with	Data for estimating SSDT difference	Number or length of comparison	Correlation coefficent	Data used	Length (year)	Mean transport (Sv)	
Oyashio off Hokkaido	GT (0–3000 m) from CTD	Satellite altimetry	12 cases	0.93	Satellite altimetry	9	–9.5	ITO et al. (2004)
Kuroshio off Enshu-nada	GT (0–1000 m) from reversing bottles	Surface GT from reversing bottles	22 years	0.77	—	—	—	NITANI (1975)
Kuroshio off Shikoku (1)	AGT (0–1000 m) from CTD/XBT & CM	Surface AGV from CTD/XBT & CM	25 cases	0.90	Satellite altimetry	7	57	IMAWAKI et al. (2001)
Kuroshio off Shikoku (2)	Temporal-mean net GT (0–1800 m) between the coast and CTD station	Temporal-mean surface geostrophic velocity	14 years	0.99	Satellite altimetry	31	61	UCHIDA (2025) & IMAWAKI et al. (2025)
Kuroshio at Tokara Strait	Transport from ferryboat-mounted ADCP	Tide gauge	9 years	0.77 (north) 0.65 (south)	Tide gauge	15	23	LIU et al. (2021)
Kuroshio in East China Sea	Proxy AGT from CPIES	Satellite altimetry	13 months	0.88	Satellite altimetry	12	19	ANDRES et al. (2008)
Ryukyu Current off Okinawa	Proxy GT from PIES	Satellite altimetry & tide gauge	9 months	0.91	Satellite altimetry & tide gauge	9	4.5	ZHU et al. (2004)
Kuroshio off Taiwan (1)	Transport from CM, moored-ADCP & CTD	Tide gauge	20 months	0.91	—	—	—	YANG et al. (2001)
Kuroshio off Taiwan (2)	Transport from CM, moored-ADCP & CTD	Satellite altimetry	20 months	0.83	Satellite altimetry	20	21	YAN & SUN (2015)

Table A1. (*continued*)

Flow in South China Sea	Proxy GT from PIES	Satellite altimetry	22 months	0.90	Satellite altimetry	22	–1.6	ZHU et al. (2015)
Atlantic inflow through Faroe-Shetland Channel	Vertically averaged velocity from moored-ADCP	Surface velocity from moored-ADCP	13 years	0.98	Satellite altimetry	19	Not estimated	BERX et al. (2013)
Gulf Stream off Cape Cod	AGT (0–1000 m) from CTD/ lowered-ADCP	Surface AGV from CTD/ lowered-ADCP	9 cases	0.96	Satellite altimetry	7	88	BREARLEY (2010)
Yucatan Channel flow	Transport from moored-ADCP & CM	Satellite altimetry	5 years	0.63	Satellite altimetry	20	Not shown	ATHIÉ et al., 2015
Florida Current (1)	Transport from submarine cable & CM	Pressure gauges	29 cases	0.97	—	—	—	MAUL et al. (1985)
Florida Current (2)	Transport from submarine cable	Satellite altimetry	7 years	0.79	Satellite altimetry	28	31	VOLKOV et al. (2020)
Brazil Current	GT (0-500 m) from XBT	Satellite altimetry	13 years	0.64	Satellite altimetry	13	–4.1	GOES et al. (2019)
Agulhas Current	Transport from CM, moored-ADCP & CPIES	Satellite altimetry	3 years	0.71–0.90	Satellite altimetry	22	Not shown	BEAL et al. (2016)

ADCP: acoustic Doppler current profiler; AGV: absolute geostrophic velocity; CPIES: current- and pressure-recording IES; PIES: pressure-recording IES altimetry data (ITO et al., 2004). They derived a nine-year-long proxy time series. KURODA et al. (2017) derived linear regressions between GTs estimated from CTD sections southeast of Hokkaido and SSDT differences estimated from gridded altimetry data. They examined horizontal structure of transport in detail.

For the Kuroshio off Enshu-nada (south of Honshu), a linear relationship was identified between GT (referred to 1000 dbar) and sea-surface GT, both estimated from hydrographic surveys using reversing bottles and a mechanical bathythermograph, together with velocity measurements using a geomagnetic electro-kinetograph (NITANI, 1975). For the Kuroshio passing through the Tokara Strait, linear relationships between volume transport estimated from ferry-mounted ADCP data and SSDT difference derived from tide gauge records were confirmed separately for the northern and southern parts of the Strait (LIU et al., 2021). They produced a 15-year-long proxy time series. For the Kuroshio in the East China Sea, ANDRES et al. (2008) confirmed a linear relationship between proxy AGT estimated from a current- and pressure-recording IES (CPIES) array, and SSDT difference estimated from altimetry data at two locations along a TOPEX/Poseidon subsatellite track. Their study yielded a 12-year-long proxy time series.

For the Ryukyu Current southeast of Okinawa, a linear relationship was confirmed between proxy GT (referred to 2000 dbar) derived from a PIES array and SSDT difference estimated from altimetry data at a point of subsatellite track and tide gauge data (ZHU et al., 2004). A nine-year-long proxy time series of GT was derived.

For the Kuroshio east of Taiwan, three studies were carried out by using Kuroshio transport data obtained by JOHNS et al. (2001) and LEE et al. (2001), as described in Section 6. A linear relationship was observed between the Kuroshio transport and SSDT difference across the East Taiwan Channel; to estimate the SSDT difference, tide gauge data at three stations located west of the Channel were examined (YANG et al., 2001). YAN and SUN (2015) identified a pair of end-points on subsatellite tracks (for estimating SSDT difference) that provided the best correlation between the transport and altimetric SSDT difference. They derived a 20-year-long proxy time series. SHEN et al. (2014) proposed a frequency-dependent transfer function from SSDT difference to transport, as an alternative more realistic than a simple linear relationship, incorporating altimetry data, a numerical model, and the Kuroshio transport data.

For the flow at the western boundary of the northern South China Sea, a linear relationship was confirmed between proxy GT estimated from a PIES array along the Jason-1/2 subsatellite track, and SSDT difference estimated from altimetry data (ZHU et al., 2015). They yielded a 22-year-long proxy time series.

For the Indonesian Throughflow, where flows differed above and below 150 m depth, SPRINTALL and RÉVELARD (2014) developed a linear, time-lagged partial regression model between transports estimated from both moored-ADCPs and CMs, and SSDT anomalies in various regions estimated from gridded altimetry data, for three years. They derived an 18-year-long proxy time series.

The East Australian Current in the South Pacific exhibited high variability due to relatively strong mesoscale eddy activity, and a simple linear relationship was not confirmed. RIDGWAY et al. (2008) constructed a 13-year-long time series of net GT between Sydney and Wellington using a combination of XBT, CTD, and altimetry data. They suggested that new, relatively inexpensive technologies, such as deepwater gliders, would be required for future AGT estimates, because large-scale field programs were unlikely to be undertaken. ZILBERMAN et al. (2018) proposed a more sophisticated method for estimating time series of AGT, by combining repeated high-density XBT transects, Argo float data (temperature, salinity, and trajectory), altimetry data, and historical hydrography data.

For the Atlantic inflow through the Faroe-Shetland Channel in the northern North Atlantic, very strong linear relationships were identified, with an average CC of 0.98 for eight sites, between vertically averaged velocity and sea-surface velocity, both estimated from a moored-ADCP array positioned along a TOPEX/Poseidon subsatellite track during 1998–2011 (BERX et al., 2013). They derived a 19-year-long proxy time series from altimetry data.

For the Gulf Stream southeast of the Cape Cod, BREARLEY (2010) observed a strong CC of 0.96 for nine comparisons between AGT in the upper 1000 m and SSDT difference. Both quantities were estimated from CTD sections with lowered-ADCP along a Jason-1 subsatellite track during 2003–2008. They derived a seven-year-long proxy time series from altimetry data.

In the case of the Florida Current, a strong linear relationship (CC of 0.97) was found for 29 comparisons between transport estimated from both an electromagnetic cable and moored CMs, and sea-level difference across the current estimated from pressure gauge data (MAUL et al., 1985). VOLKOV et al. (2020) confirmed this linear relationship using transport estimated from a decommissioned submarine cable and SSDT difference estimated from altimetry data at two segments of a subsatellite track. They derived a 28-year-long proxy time series.

For the Yucatan Channel flow from the Caribbean Sea to the Gulf of Mexico, a linear relationship was confirmed between transport estimated from both moored-ADCP and CM array data for five years, and SSDT difference estimated from gridded altimetry data at two locations (ATHIÉ et al., 2015). They constructed a 20-year-long proxy time series.

In numerical models for the Atlantic Ocean, HIRSCHI et al. (2009) found a significant correlation between meridional volume transport in the upper 1100 m and zonal SSDT difference, provided that transport in the western-boundary current region and that in the eastern part of the basin were considered separately.

For the Brazil Current at 22° S in the South Atlantic, GOES et al. (2019) confirmed a linear relationship between GT estimated from repeated high-density XBT transects and SSDT difference estimated from gridded altimetry data. They derived a 13-year-long proxy time series.

For the Benguela Current in the eastern South Atlantic, west of South Africa, GARZOLI et al. (1997) found a significant correlation between SSDT anomalies estimated from along-track altimetry data and proxy sea-surface dynamic height derived from IES data, from which GT in the upper 1000 m can be estimated by using an empirically determined constant. They derived a three-year-long proxy time series.

For the Agulhas Current, VAN SEBILLE et al. (2010) confirmed a linear relationship between transport and SSDT difference, using a regional numerical model, prior to large-scale observational efforts. Subsequently, BEAL et al. (2015) deployed a moored-instrument array, heavily equipped with CMs, ADCPs, and CPIESs, along a Jason-1/2 subsatellite track during 2010–2013, to obtain time series of volume transport. Based on those field data, BEAL and ELIPOT (2016) developed linear regression models between transport per unit distance and sea-surface slope. They constructed a 22-year-long proxy time series from altimetry data.

For the Antarctic Circumpolar Current at 140°E, Rintoul et al. (2002) found an exceptionally strong one-to-one relationship between GT (referred to 2500 dbar) integrated northward from the southern end to a given latitude, and SSDT at that latitude. Both quantities were estimated from six repeated CTD sections conducted during the 1990s. They derived a six-year-long proxy time series from gridded altimetry data. For that Current in the Drake Passage, where temporal and spatial variability of narrow fronts were important, Koenig et al. (2014) constructed a look-up table for vertical velocity profiles as functions of latitude and sea-surface velocity, based on data from a three-year moored-CM array positioned along a Jason-1 subsatellite track. They derived a 20-year-long proxy time series of full-depth volume transport from altimetry data.

Acknowledgements

As a coordinator of the ASUKA (Affiliated Surveys of the Kuroshio off Cape Ashizuri) Group, the author expresses his profound gratitude to all the scientists, technicians, captains and crew members, supporting staff, and students who contributed to the ASUKA observation in their various ways. Without their efforts, the ASUKA observation would not have been successful. Especially, the author is indebted to core members Hiroshi Ichikawa, Masao Fukasawa, Hiroshi Uchida, and Shin-ichiro Umatani for their contributions to making the plan, implementing it, and producing the results. He also thanks two anonymous reviewers for their valuable comments based on very careful reading of the manuscript. The ASUKA intensive observation was financially supported by the former Ministry of Education, Science, Sports and Culture (Japan), the Office of Naval Research (United States of America), and other funding sources. This study is a contribution to the WOCE (World Ocean Circulation Experiment). Metadata for the current-meter data obtained during the ASUKA intensive observation, including stick diagrams of daily current vectors, are available at: https://www.riam.kyushu-u.ac.jp/oed/asuka/cm/index.html, and data themselves are available at: https://www.cmrecords.net/cmdac/stranger/pcm5/pcm5.html. The hydrographic data obtained by the ASUKA Group are available at: https://www.riam.kyushu-u.ac.jp/oed/asuka/ahdc/index.html. The data for proxy time series of geostrophic transport for the Kuroshio and the throughflow Kuroshio across the ASUKA section for 1992–2024 are provided in Online Resource 2 of Imawaki et al. (2025).

References

Amante, C. and B.W. Eakins (2009): ETOPO1 1 Arc-Minute Global Relief Model: Procedures, Data Sources and Analysis, NOAA Technical Memorandum NESDIS NGDC-24. National Geophysical Data Center, NOAA. https://doi.org/10.7289/V5C8276M

Ando, K., X. Lin, C. Villanoy et al. (2021): Half-century of scientific advancements since the Cooperative Study of the Kuroshio and Adjacent Regions (CSK) programme — Need for a new Kuroshio research. Prog. Oceanogr., **193**, 102513. https://doi.org/10.1016/j.pocean.2021.102513

Andres, M., J.-H. Park, M. Wimbush, X.-H. Zhu, K.-I. Chang and H. Ichikawa (2008): Study of the Kuroshio/Ryukyu Current system based on satellite-altimeter and *in situ* measurements. J. Oceanogr., **64**, 937-950. https://doi.org/10.1007/s10872-008-0077-2

Athié, G., J. Sheinbaum, R. Leben, J. Ochoa, M.R. Shannon and J. Candela (2015): Interannual variability in the Yucatan Channel flow. Geophys. Res. Lett., **42**, 1496-1503. https://doi.org/10.1002/2014GL062674

AVISO (2016): SSALTO/DUACS User Handbook:

MSLA and (M) ADT Near-Real Time and Delayed Time Products. http://www.aviso.altimetry.fr/fileadmin/documents/data/tools/hdbk_duacs.pdf

Beal, L.M., T.K. Chereskin, Y.D. Lenn and S. Elipot (2006): The sources and mixing characteristics of the Agulhas Current. J. Phys. Oceanogr., **36**, 2060-2074. https://doi.org/10.1175/JPO2964.1

Beal, L.M. and S. Elipot (2016): Broadening not strengthening of the Agulhas Current since the early 1990s. Nature, **540**, 570-573. https://doi.org/10.1038/nature19853

Beal, L.M., S. Elipot, A. Houk and G.M. Leber (2015): Capturing the transport variability of a western boundary jet: Results from the Agulhas Current Time-Series Experiment (ACT). J. Phys. Oceanogr., **45**, 1302-1324. https://doi.org/10.1175/JPO-D-14-0119.1

Berx, B., B. Hansen, S. Østerhus, K.M. Larsen, T. Sherwin and K. Jochumsen (2013): Combining in situ measurements and altimetry to estimate volume, heat and salt transport variability through the Faroe-Shetland Channel. Ocean Science, **9**, 639-654. https://doi.org/10.5194/os-9-639-2013

Book, J.W., M. Wimbush, S. Imawaki, H. Ichikawa, H. Uchida and H. Kinoshita (2002a): Kuroshio temporal and spatial variations south of Japan determined from inverted echo sounder measurements. J. Geophys. Res., **107**, 3121. https://doi.org/10.1029/2001JC000795

Book, J., et al. (2002b): Correction to "Kuroshio temporal and spatial variations south of Japan determined from inverted echo sounder measurements" by J. Book et al. J. Geophys. Res., **107**, 3234. https://doi.org/10.1029/2002JC001678

Brearley, J.A. (2010): Upper ocean transport variability in the subtropical North Atlantic. University of Southampton, School of Ocean and Earth Science, Doctoral Thesis, 303 pp. https://eprints.soton.ac.uk/191959/

Bryden, H.L., L.M. Beal and L.M. Duncan (2005): Structure and transport of the Agulhas Current and its temporal variability. J. Oceanogr., **61**, 479-492. https://doi.org/10.1007/s10872-005-0057-8

Bryden, H.L. and M.M. Hall (1980): Heat transport by currents across 25° N latitude in the Atlantic Ocean. Science, **207**, 884-886. https://doi.org/10.1126/science.207.4433.884

Bryden, H.L. and S. Imawaki (2001): Ocean heat transport. *In* Ocean Circulation and Climate: Observing and Modelling the Global Ocean. Siedler, G., J. Church and J. Gould (eds.), Academic Press, San Diego, International Geophysics Series, Volume 77, p. 455-474.

Bryden, H.L., D.H. Roemmich and J.A. Church (1991): Ocean heat transport across 24° N in the Pacific. Deep-Sea Res., **38**, 297-324. https://doi.org/10.1016/0198-0149(91)90070-V

Chen, S., B. Qiu and P. Hacker (2007): Profiling float measurements of the recirculation gyre south of the Kuroshio Extension in May to November 2004. J. Geophys. Res., **112**, C05023. https://doi.org/10.1029/2006JC004005

Clarke, A., J. Church and J. Gould (2001): Ocean processes and climate phenomena. *In* Ocean Circulation and Climate: Observing and Modelling the Global Ocean. Siedler, G., J. Church and J. Gould (eds.), Academic Press, San Diego, International Geophysics Series, Volume 77, p. 11-30.

Escudier, P., A. Couhert, F. Mercier et al. (2017): Satellite radar altimetry: Principle, accuracy, and precision. *In* Satellite Altimetry over Oceans and Land Surfaces. Stammer, D. and A. Cazenave (eds.), CRC Press, London, p. 1-69.

Flament, P. (2002): A state variable for characterizing water masses and their diffusive stability: Spiciness. Prog. Oceanogr., **54**, 493-501. https://doi.org/10.1016/S0079-6611(02)00065-4

Fu, L.-L., E.J. Christensen, C.A. Yamarone Jr., M. Lefebvre, Y. Menard, M. Dorrer and P. Escudier (1994): TOPEX/POSEIDON mission overview. J. Geophys. Res., **99**, 24,369-24,381. https://doi.org/10.1029/94JC01761

Fujio, S., D. Yanagimoto and K. Taira (2000): Deep current structure above the Izu-Ogasawara Trench. J. Geophys. Res., **105**, 6377-6386. https://doi.org/10.1029/1999JC900324

Fukasawa, M., T. Teramoto and K. Taira (1987):

Abyssal current along the northern periphery of Shikoku Basin. J. Oceanogr. Soc. Japan, **42**, 459-472. https://doi.org/10.1007/BF02110196

Fukasawa, M., T. Teramoto and K. Taira (1995): Hydrographic structure in association with deep boundary current in the north of the Shikoku Basin. J. Oceanogr., **51**, 187-205. https://doi.org/10.1007/BF02236524

Garzoli, S.L., G.J. Goñi, A.J. Mariano and D.B. Olson (1997): Monitoring the upper southeastern Atlantic transports using altimeter data. J. Mar. Res., **55**, 453-481. https://elischolar.library.yale.edu/journal_of_marine_research/2231

Goes, M., M. Cirano, M. M. Mata and S. Majumder (2019): Long-term monitoring of the Brazil Current transport at 22° S from XBT and altimetry data: Seasonal, interannual, and extreme variability. J. Geophys. Res. Oceans, **124**, 3645-3663. https://doi.org/10.1029/2018JC014809

Grassl, H. (2001): Climate and oceans. *In* Ocean Circulation and Climate: Observing and Modelling the Global Ocean. Siedler, G., J. Church and J. Gould (eds.), Academic Press, San Diego, International Geophysics Series, Volume 77, p. 3-9.

Guo, X.Y., X.-H. Zhu, Y. Long and D.J. Huang (2013): Spatial variations in the Kuroshio nutrient transport from the East China Sea to south of Japan. Biogeosciences, **10**, 6403-6417. https://doi.org/10.5194/bg-10-6403-2013

Guo, X., X.-H. Zhu, Q.-S. Wu and D. Huang (2012): The Kuroshio nutrient stream and its temporal variation in the East China Sea. J. Geophys. Res., **117**, C01026. https://doi.org/10.1029/2011JC007292

Halkin, D. and T. Rossby (1985): The structure and transport of the Gulf Stream at 73° W. J. Phys. Oceanogr., **15**, 1439-1452. https://doi.org/10.1175/1520-0485(1985)015<1439:TSATOT>2.0.CO;2

Hasunuma, K. and K. Yoshida (1978): Splitting of the subtropical gyre in the western North Pacific. J. Oceanogr. Soc. Japan, **34**, 160-172. https://doi.org/10.1007/BF02108654

Heiderich, J. and R.E. Todd (2020): Along-stream evolution of Gulf Stream volume transport. J. Phys. Oceanogr., **50**, 2251-2270. https://doi.org/10.1175/JPO-D-19-0303.1

Hirschi, J.J-M., P.D. Killworth, J.R. Blundell and D. Cromwell (2009): Sea surface height signals as indicators for oceanic meridional mass transports. J. Phys. Oceanogr., **39**, 581-601. https://doi.org/10.1175/2008JPO3923.1

Ichikawa, H., H. Nakamura, A. Nishina and M. Higashi (2004): Variability of northeastward current southeast of northern Ryukyu Islands. J. Oceanogr., **60**, 351-363. https://doi.org/10.1023/B:JOCE.0000038341.27622.73

Imawaki, S., A.S. Bower, L. Beal and B. Qiu (2013): Western boundary currents. *In* Ocean Circulation and Climate: A 21st Century Perspective. Siedler, G., S. M. Griffies, J. Gould and J. A. Church (eds.), Academic Press, London, International Geophysics Series, Volume 103, p. 305-338.

Imawaki, S. and H. Uchida (1995): Detecting sea level profiles across the Kuroshio by a satellite altimeter. Annuals of the Disaster Prevention Research Institute, Kyoto University, **38B-2**, 655-662 (in Japanese with English abstract). http://hdl.handle.net/2433/72595

Imawaki, S., H. Uchida, H. Ichikawa, M. Fukasawa, S. Umatani and ASUKA Group (1997): Time series of the Kuroshio transport derived from field observations and altimetry data. Intl. WOCE Newsletter, **25**, 15-18.

Imawaki, S., H. Uchida, H. Ichikawa, M. Fukasawa, S. Umatani and the ASUKA Group (2001): Satellite altimeter monitoring the Kuroshio transport south of Japan. Geophys. Res. Lett., **28**, 17-20. https://doi.org/10.1029/2000GL011796

Imawaki, S., H. Uchida, H. Ichikawa, M. Fukasawa, S. Umatani and H. Yoritaka (2023): Volume transport of the Kuroshio south of Japan estimated from repeated full-depth hydrographic surveys and current measurements. J. Oceanogr., **79**, 157-183. https://doi.org/10.1007/s10872-022-00672-3

Imawaki, S., H. Uchida, Y.-X. Qiao and H. Nakamura (2025): Kuroshio volume transport over the past 3 decades estimated from combined satellite altimetry and hydrography data. J. Oceanogr.,

81, 351-359. https://doi.org/10.1007/s10872-025-00756-w

Isobe, A. and S. Imawaki (2001): Annual variation of the Kuroshio transport in a two-layer numerical model with a ridge. J. Phys. Oceanogr., **32**, 994-1009. https://doi.org/10.1175/1520-0485(2002)032<0994:AVOTKT>2.0.CO;2

Ito, S., K. Uehara, T. Miyao, H. Miyake, I. Yasuda, T. Watanabe and Y. Shimizu (2004): Characteristics of SSH anomaly based on TOPEX/POSEIDON altimetry and *in situ* measured velocity and transport of Oyashio on OICE. J. Oceanogr., **60**, 425-437. https://doi.org/10.1023/B:JOCE.0000038059.54334.6b

Johns, W.E., T.N. Lee, D. Zhang, R. Zantopp, C.-T. Liu and Y. Yang (2001): The Kuroshio east of Taiwan: Moored transport observations from the WOCE PCM-1 array. J. Phys. Oceanogr., **31**, 1031-1053. https://doi.org/10.1175/1520-0485(2001)031<1031:TKEOTM>2.0.CO;2

Johns, W.E., T.J. Shay, J.M. Bane and D.R. Watts (1995): Gulf Stream structure, transport, and recirculation near 68° W. J. Geophys. Res., **100**, 817-838. https://doi.org/10.1029/94JC02497

Kakinoki, K., S. Imawaki, K. Ichikawa, S. Umatani and M. Kashima (2008a): Variations of velocity and transport associated with coastal cyclonic eddies off Shikoku, Japan estimated from moored current meter and IES data. Reports of Research Institute for Applied Mechanics, Kyushu University, No.**135**, 53-59 (in Japanese with English abstract). https://doi.org/10.15017/14184

Kakinoki, K., S. Imawaki, H. Uchida, H. Nakamura, K. Ichikawa, S. Umatani, A. Nishina, H. Ichikawa and M. Wimbush (2008b): Variations of Kuroshio geostrophic transport south of Japan estimated from long-term IES observations. J. Oceanogr., **64**, 373-384. https://doi.org/10.1007/s10872-008-0030-4

Kaneko, A., S. Mizuno, W. Koterayama and R.L. Gordon (1992): Cross-stream velocity structures and their downstream variation of the Kuroshio around Japan. Deep-Sea Res., **39**, 1583-1594. https://doi.org/10.1016/0198-0149(92)90049-Y

Kaneko, I., Y. Takatsuki and H. Kamiya (2001): Circulation of intermediate and deep waters in the Philippine Sea. J. Oceanogr., **57**, 397-420. https://doi.org/10.1023/A:1021565031846

Kashima, M., S. Imawaki, S. Umatani, H. Uchida, Y. Hashibe, H. Ichikawa and M. Fukasawa (2003): Geostrophy in the intermediate and deep layers of the Kuroshio and its recirculation regions south of Japan. J. Oceanogr., **59**, 291-301. https://doi.org/10.1023/A:1025559709293

Kashima, M., S. Ito, K. Ichikawa, S. Imawaki, S. Umatani, H. Uchida and T. Setou (2009): Quasiperiodic small meanders of the Kuroshio off Cape Ashizuri and their inter-annual modulation caused by quasiperiodic arrivals of mesoscale eddies. J. Oceanogr., **65**, 73- 80. https://doi.org/10.1007/s10872-009-0007-y

Kawabe, M. (1985): Sea level variations at the Izu Islands and typical stable paths of the Kuroshio. J. Oceanogr. Soc. Japan, **41**, 307-326. https://doi.org/10.1007/BF02109238

Kawabe, M. (1995): Variations of current path, velocity, and volume transport of the Kuroshio in relation with the large meander. J. Phys. Oceanogr., **25**, 3103-3117. https://doi.org/10.1175/1520-0485(1995)025<3103:VOCPVA>2.0.CO;2

Koenig, Z., C. Provost, R. Ferrari, N. Sennéchael and M.-H. Rio (2014): Volume transport of the Antarctic Circumpolar Current: Production and validation of a 20 year long time series obtained from in situ and satellite observations. J. Geophys. Res. Oceans, **119**, 5407-5433. https://doi.org/10.1002/2014JC009966

Kuroda, H., T. Wagawa, S. Kakehi, Y. Shimizu, A. Kusaka, T. Okunishi, D. Hasegawa and S. Ito (2017): Long-term mean and seasonal variation of altimetry-derived Oyashio transport across the A-line off the southeastern coast of Hokkaido, Japan. Deep-Sea Res. I, **121**, 95-109. https://doi.org/10.1016/j.dsr.2016.12.006

Leaman, K.D., E. Johns and T. Rossby (1989): The average distribution of volume transport and potential vorticity with temperature at three sections across the Gulf Stream. J. Phys. Oceanogr., **19**, 36-51. https://doi.org/10.1175/1520-0485(198

9)019<0036:TADOVT>2.0.CO;2

Lee, T.N., W.E. Johns, C.T. Liu, D. Zhang, R. Zantopp and Y. Yang (2001): Mean transport and seasonal cycle of the Kuroshio east of Taiwan with comparison to the Florida Current. J. Geophys. Res., **106**, 22,143-22,158. https://doi.org/10.1029/2000JC000535

Liu, Z.-J., H. Nakamura, X.-H. Zhu, A. Nishina, X. Guo and M. Dong (2019): Tempo-spatial variations of the Kuroshio current in the Tokara Strait based on long-term ferryboat ADCP data. J. Geophys. Res., **124**, 6030-6049. https://doi.org/10.1029/2018JC014771

Liu, Z.-J., X.-H. Zhu, H. Nakamura, A. Nishina, M. Wang and H. Zheng (2021): Comprehensive observational features for the Kuroshio transport decreasing trend during a recent global warming hiatus. Geophys. Res. Lett., **48**, e2021GL094169. https://doi.org/10.1029/2021GL094169

Long, Y., X.-H. Zhu, X. Guo and H. Huang (2018): Temporal variation of Kuroshio nutrient stream south of Japan. J. Geophys. Res., **123**, 7896-7913. https://doi.org/10.1029/2017JC013635

Macdonald, A.M. and M.O. Baringer (2013): Ocean heat transport. *In* Ocean Circulation and Climate: A 21st Century Perspective. Siedler, G., S.M. Griffies, J. Gould and J.A. Church (eds.), Academic Press, London, International Geophysics Series, Volume 103, p. 759-785.

Macdonald, A.M. and C. Wunsch (1996): An estimate of global ocean circulation and heat fluxes. Nature, **382**, 436-439. https://doi.org/10.1038/382436a0

Maul, G.A., F. Chew, M. Bushnell and D.A. Mayer (1985): Sea level variation as an indicator of Florida Current volume transport: Comparisons with direct measurements. Science, **227**, 304-307. https://doi.org/10.1126/science.227.4684.304

Nagano, A., T. Hasegawa, H. Matsumoto and K. Ariyoshi (2018): Bottom pressure change associated with the 2004-2005 large meander of the Kuroshio south of Japan. Ocean Dynamics, **68**, 847-865. https://doi.org/10.1007/s10236-018-1169-1

Nagano, A., K. Ichikawa, H. Ichikawa, M. Konda and K. Murakami (2009): Synoptic flow structures in the confluence region of the Kuroshio and the Ryukyu Current. J. Geophys. Res., **114**, C06007. https://doi.org/10.1029/2008JC005213

Nagano, A., K. Ichikawa, H. Ichikawa, M. Konda and K. Murakami (2013): Volume transports proceeding to the Kuroshio Extension region and recirculating in the Shikoku Basin. J. Oceanogr., **69**, 285-293. https://doi.org/10.1007/s10872-013-0173-9

Nagano, A., K. Ichikawa, H. Ichikawa, H. Tomita, H. Tokinaga and M. Konda (2010): Stable volume and heat transports of the North Pacific subtropical gyre revealed by identifying the Kuroshio in synoptic hydrography south of Japan. J. Geophys. Res., **115**, C09002. https://doi.org/10.1029/2009JC005747

Nakamura, H. (2017): Kuroshio path and volume transport variations from Luzon Island to the eastern coast of Kyushu. Oceanography in Japan, **26**, 113-147 (in Japanese with English abstract). https://kaiyo-gakkai.jp/jos/uminokenkyu/vol26/26-4/26-4-nakamura.pdf

Nakano, T., I. Kaneko and Y. Takatsuki (1994): The Kuroshio structure and transport estimated by the inverse method. J. Phys. Oceanogr., **24**, 609-618. https://doi.org/10.1175/1520-0485(1994)024<0609:TKSATE>2.0.CO;2

Nitani, H. (1975): Variation of the Kuroshio south of Japan. J. Oceanogr. Soc. Japan, **31**, 154-173. https://doi.org/10.1007/BF02107107

Otsuka, K. (1985): Characteristics of the Kuroshio in the vicinity of the Izu Ridge. J. Oceanogr. Soc. Japan, **41**, 441-451. https://doi.org/10.1007/BF02109038

Qiu, B. (2002): The Kuroshio Extension system: Its large-scale variability and role in the midlatitude ocean-atmosphere interaction. J. Oceanogr., **58**, 57-75. https://doi.org/10.1023/A:1015824717293

Qiu, B. and S. Chen (2021): Revisit of the occurrence of the Kuroshio large meander south of Japan. J. Phys. Oceanogr., **51**, 3679-3694. https://doi.org/10.1175/JPO-D-21-0167.1

Ridgway, K.R., R.C. Coleman, R.J. Bailey and P. Sutton (2008): Decadal variability of East Australian Current transport inferred from repeated high-density XBT transects, a CTD survey and satellite altimetry. J. Geophys. Res., **113**, C08039. https://doi.org/10.1029/2007JC004664

Rintoul, S.R., S. Sokolov and J. Church (2002): A 6 year record of baroclinic transport variability of the Antarctic Circumpolar Current at 140° E derived from expendable bathythermograph and altimeter measurements. J. Geophys. Res., **107** (C10), 3155. https://doi.org/10.1029/2001JC000787

Sakamoto, T. (2005): Effect of air-sea heat exchange on seasonal transport variation of the Kuroshio. J. Mar. Res., **63**, 579-600. https://elischolar.library.yale.edu/cgi/viewcontent.cgi?article=1091&context=journal_of_marine_research

Shen, M.-L., Y.-H. Tseng, S. Jan, C.-C. Young and M.-D. Chiou (2014): Long-term variability of the Kuroshio transport east of Taiwan and the climate it conveys. Prog. Oceanogr., **121**, 60-73. https://doi.org/10.1016/j.pocean.2013.10.009

Siedler, G., J. Church and J. Gould (eds.) (2001): Ocean Circulation and Climate: Observing and Modelling the Global Ocean. Academic Press, San Diego, International Geophysics Series, Volume 77, 715 pp.

Sprintall, J. and A. Révelard (2014): The Indonesian throughflow response to Indo-Pacific climate variability. J. Geophys. Res., **119**, 1161-1175. https://doi.org/10.1002/2013JC009533

Sugimoto, S., K. Hanawa, K. Narikiyo, M. Fujimori and T. Suga (2010): Temporal variations of the net Kuroshio transport and its relation to atmospheric variations. J. Oceanogr., **66**, 611-619. https://doi.org/10.1007/s10872-010-0050-8

Taft, B.A. (1972): Characteristics of the flow of the Kuroshio south of Japan. *In* Kuroshio: Its Physical Aspects. Stommel, H. and K. Yoshida (eds.), Univ. Tokyo Press, p. 165-216.

Taft, B.A. (1978): Structure of Kuroshio south of Japan. J. Mar. Res., **36**, 77-117. https://elischolar.library.yale.edu/journal_of_marine_research/1424

Takematsu, M., K. Kawatate, W. Koterayama, T. Suhara and H. Mitsuyasu (1986): Moored instrument observations in the Kuroshio south of Kyushu. J. Oceanogr. Soc. Japan, **42**, 201-211. https://doi.org/10.1007/BF02109354

Takeuchi, M., S. Imawaki, S. Umatani, K. Yamada, H. Uchida and M. Fukasawa (2002): Velocity structures of the Kuroshio and coastal cyclonic eddies off Shikoku, Japan observed by moored ADCPs. Reports of Research Institute for Applied Mechanics, Kyushu University, No.**123**, 29-38 (in Japanese with English abstract). https://doi.org/10.15017/6769081

Talley, L.D. (1984): Meridional heat transport in the Pacific Ocean. J. Phys. Oceanogr., **14**, 231-241. https://doi.org/10.1175/1520-0485(1984)014<0231:MHTITP>2.0.CO;2

Thoppil, P.G., E.J. Metzger, H.E. Hurlburt, O.M. Smedstad and H. Ichikawa (2016): The current system east of the Ryukyu Islands as revealed by a global ocean reanalysis. Prog. Oceanogr., **141**, 239-258. https://doi.org/10.1016/j.pocean.2015.12.013

Uchida, H. (2025): The Kuroshio transport time series estimated from satellite altimeter data. JAMSTEC. https://doi.org/10.17596/0004021

Uchida, H. and S. Imawaki (2008): Estimation of the sea level trend south of Japan by combining satellite altimeter data with in situ hydrographic data. J. Geophys. Res., **113**, C09035. https://doi.org/10.1029/2008JC004796

Uchida, H., S. Imawaki, H. Ichikawa and the ASUKA Group (2008): ASUKA Hydrographic Data Collection. Reports of Research Institute for Applied Mechanics, Kyushu University, No.**135**, 21-31. https://doi.org/10.15017/14180

Umatani, S., M. Kashima, S. Imawaki, H. Ichikawa and M. Fukasawa (2001): Structures and variability of the Kuroshio off Shikoku, Japan revealed by direct current measurements. Reports of Research Institute for Applied Mechanics, Kyushu University, No.**121**, 87-94 (in Japanese with English abstract). https://doi.org/10.15017/6768408

van Sebille, E., L.M. Beal and A. Biastoch (2010): Sea surface slope as a proxy for Agulhas Current strength. Geophys. Res. Lett., **37**, L09610.

https://doi.org/10.1029/2010GL042847

Volkov, D.L., R. Domingues, C.S. Meinen, R. Garcia, M. Baringer, G. Goni and R.H. Smith (2020): Inferring Florida Current volume transport from satellite altimetry. J. Geophys. Res., **125**, e2020JC016763. https://doi.org/10.1029/2020JC016763

Wei, Y., D. Huang and X.-H. Zhu (2013): Interannual to decadal variability of the Kuroshio Current in the East China Sea from 1955 to 2010 as indicated by in-situ hydrographic data. J. Oceanogr., **69**, 571-589. https://doi.org/10.1007/s10872-013-0193-5

Wijffels, S.E., M.M. Hall, T. Joyce, D.J. Torres, P. Hacker and E. Firing (1998): Multiple deep gyres of the western North Pacific: A WOCE section along 149° E. J. Geophys. Res., **103**, 12,985-13,009. https://doi.org/10.1029/98JC01016

Worthington, L.V. and H. Kawai (1972): Comparison between deep sections across the Kuroshio and the Florida Current and Gulf Stream. *In* Kuroshio: Its Physical Aspects. Stommel, H. and K. Yoshida (eds.), Univ. Tokyo Press, p. 371-385.

Wunsch, C. (1978): The North Atlantic general circulation west of 50° W determined by inverse methods. Rev. Geophys., **16**, 583-620. https://doi.org/10.1029/RG016i004p00583

Yan, X. and C. Sun (2015): An altimetric transport index for Kuroshio inflow northeast of Taiwan Island. Science China Earth Sciences, **58**, 697-706. https://doi.org/10.1007/s11430-014-5024-z

Yang, Y., C.-T. Liu, T.N. Lee, W. Johns, H.-W. Li and M. Koga (2001): Sea surface slope as an estimator of the Kuroshio volume transport east of Taiwan. Geophys. Res. Lett., **28**, 2461-2464. https://doi.org/10.1029/2000GL011709

You, Y., N. Suginohara, M. Fukasawa, H. Yoritaka, K. Mizuno, Y. Kashino and D. Hartoyo (2003): Transport of North Pacific Intermediate Water across Japanese WOCE sections. J. Geophys. Res., **108**, 3196. https://doi.org/10.1029/2002JC001662

Zhang, Z.-L., H. Nakamura and X.-H. Zhu (2021): Seasonal velocity variations over the entire Kuroshio path part II: Dynamical interpretation for the current speed variation. J. Oceanogr., **77**, 745-761. https://doi.org/10.1007/s10872-021-00603-8

Zhao, R., H. Nakamura, X.-H. Zhu, J.-H. Park, A. Nishina, C. Zhang, H. Na, C. Jeon, Z.-N. Zhu and H.S. Min (2020): Tempo-spatial variations of the Ryukyu Current southeast of Miyakojima Island determined from mooring observations. Science Rep., **10**, 6656. https://doi.org/10.1038/s41598-020-63836-5

Zhu, X.-H., H. Ichikawa, K. Ichikawa and K. Takeuchi (2004): Volume transport variability southeast of Okinawa Island estimated from satellite altimeter data. J. Oceanogr., **60**, 953-962. https://doi.org/10.1007/s10872-005-0004-8

Zhu, X.-H., A. Kaneko, T. Saito and N. Gohda (2001): Kuroshio stream path variation and its associated velocity structures south of Shikoku, Japan. Geophys. Res. Lett., **28**, 4615-4618. https://doi.org/10.1029/2001GL013730

Zhu, X.-H., J.-H. Park and I. Kaneko (2006): Velocity structures and transports of the Kuroshio and the Ryukyu Current during fall of 2000 estimated by an inverse technique. J. Oceanogr., **62**, 587-596. https://doi.org/10.1007/s10872-006-0078-y

Zhu, X.-H., R. Zhao, X. Guo, Y. Long, Y.-L. Ma and X. Fan (2015): A long-term volume transport time series estimated by combining in situ observation and satellite altimeter data in the northern South China Sea. J. Oceanogr., **71**, 663-673. https://doi.org/10.1007/s10872-015-0305-5

Zilberman, N.V., D.H. Roemmich, S.T. Gille and J. Gilson (2018): Estimating the velocity and transport of western boundary current systems: A case study of the East Australian Current near Brisbane. J. Atmos. Oceanic Technol., **35**, 1313-1329. https://doi.org/10.1175/JTECH-D-17-0153.1

Received: March 14, 2025
Accepted: June 27, 2025